Validation of Outgoing Longwave Radiation Product derived from INSAT-3D IMAGER Payload for the period 2014-2019

Amit Kumar, S. K. Mukherjee, R.K. Giri, Virendra Singh

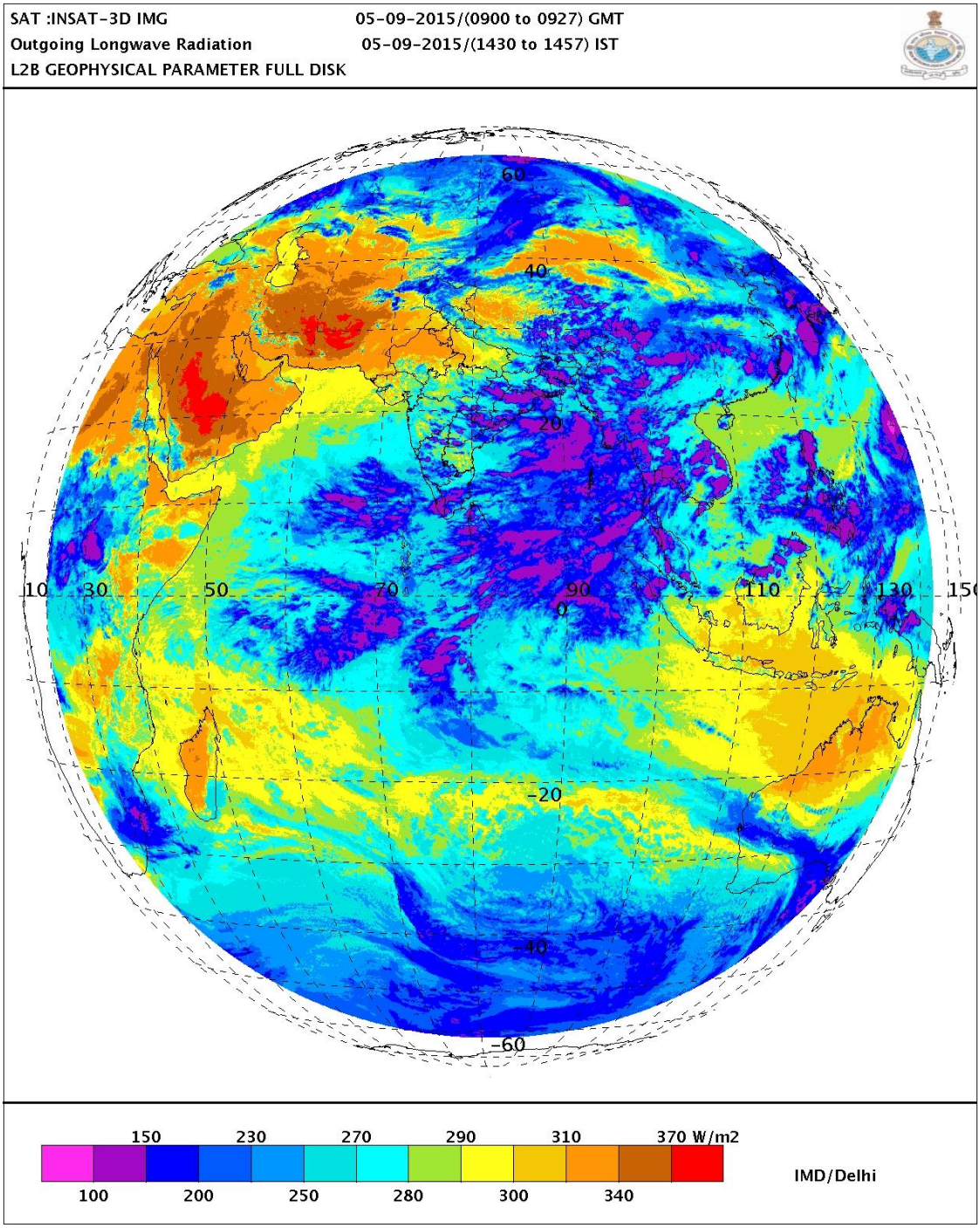

National Meteorological Satellite Centre,

India Meteorological Department

September, 2019

INDIA METEOROLOGICAL DEPARTMENT (IMD)

Report Number:	**ESSO/IMD/SATMET/02/2019/10**
Title of the Report:	Validation of Outgoing Longwave Radiation Product derived from INSAT-3D IMAGER Payload for the period 2014-2019
Author(s):	Amit Kumar, S. K. Mukherjee, R.K. Giri, Virendra Singh
Type of document:	Scientific Report
Number of pages, figures & tables:	39, 06 & 06
Reviewing and approving Authority:	Director General of Meteorology, IMD
Security classification:	Unclassified
Distribution:	Unrestricted
Date of publication:	13.09.2019

ACKNOWLEDGEMENTS

The authors express their sincere thanks to Secretary Ministry of Earth Sciences (MOES), Secretary and Chairman, Indian Space Research Organisation (ISRO), Director General of Meteorology (IMD) and Director Space Application Centre (SAC), Ahmedabad for their continued encouragement and support for carrying out Validation of Outgoing Longwave Radiation Product from INSAT-3D IMAGER Payload. The authors express their sincere thanks to all the organisations like IMD (Satellite Division), SAC, ISRO & officials involved in the activity, for their active co-operation. We also thank the officers and staff of Satellite Division and SAC for their valuable contribution and guidance in bringing out the validation report.

Amit Kumar

Contents

Chapter 1. Introduction ---------- 03

Chapter 2. Data and methodology ---------- 5

Chapter 3. Results & Discussion ---------- 7

Chapter 4. Summary and conclusions ---------- 12

References ---------- 13

Tables & Figures ---------- 14

1. **Introduction**

Outgoing longwave radiation (OLR) is a major component of Earth's radiation budget and it represents the total amount of radiation emitted from earth atmosphere system to the outer space. The top of the atmosphere radiative energy balance between net incoming solar radiation and OLR is crucial in determining the large-scale atmospheric circulation and, therefore, the synoptic evolution that is important for weather and climate prediction. Since long, OLR has been estimated for variety of problems in climate sensitivity and diagnostics (Schmetz and Liu, 1988), numerical weather forecasting and climate models. OLR varies inversely with the cloud top temperature resulting low radiation values from convective systems. OLR has been estimated by satellite instruments since 1974 making it one the longest available satellite based records for any geophysical parameters. Many dedicated broadband instruments are flown over satellites for measuring OLR like, Earth Radiation Budget Experiment (ERBE), Scanner Radiometer for Radiation Budget (ScaRab) and Cloud and Earth's Radiant Energy System (CERES) etc. In addition to these many algorithms are also developed for estimating OLR by converting the narrowband radiance observations into broadband flux (Gruber and Winston, 1978; Ellingson and Ferraro, 1983; Gruber and Krueger, 1984). Ellingson et al. (1989) have shown that the linear combination of only four (6.6-6.9 μm; 7.9-8.5 μm; 13.1-13.6 μm; 14.3-14.7 μm) High Resolution Infrared Sounder (HIRS) channels could account for more than 99% of the OLR total variance. Schmetz and Liu (1988) and Cheruy et al. (1991) developed OLR retrieval technique using

two channels (infrared window and water vapor) of Meteosat. Minnis et al. (1991) developed an algorithm to estimate OLR using Geostationary Operational Environmental Satellite (GOES) imager window channels with additional water vapor information from analysis. Ba and Ellingson (2001) estimated OLR using several channels of the GOES sounder and presented comparisons with the CERES measurements. Ba et al. (2003) and Lee et al. (2004) adapted the HIRS OLR technique to GOES sounder. Singh et al. (2007) estimated OLR using the infrared window and water vapor channels radiances from Kalpana satellite. Various studies (Ellingson et al., 1994; Gruber et al., 1994; Lee et al., 2007) have been caries out to validate these OLR estimates with broadband observations obtained from ERBE and CERES.

The primary goal of this study is to evaluate the performance of INSAT-3D satellite derived Outgoing longwave radiation. This is achieved by comparing INSAT derived Outgoing longwave radiation against Clouds and the Earth's Radiant Energy System (CERES) on board Suomi NPP (National Polar-orbiting Partnership) for the period February 2014 to June 2019.

Chapter 2 Data and methodology

INSAT-3D OLR data

INSAT-3D Outgoing longwave radiation (OLR) is generated operationally at INSAT Meteorological Data Processing System (IMDPS), New Delhi at pixel resolution (5KM at nadir) and at half-hourly interval. OLR is estimated from narrow band radiances from WV (6.5-7.1 μm), TIR-1 (10.2-11.3 μm) and TIR-2 (11.5-12.5 μm) channels of INSAT-3D imager (Singh et al., 2013; OLR ATBD 10.19038/SAC/10/3DIMG_L2B_OLR). The product dimension is 20°E to 130° E and 60°S to 60°N.

Clouds and the Earth's Radiant Energy System (CERES) data

The Clouds and the Earth's Radiant Energy System is a key instrument [Flight Model (FM) 5] is placed on board the Suomi National Polar-orbiting Partnership (NPP) satellite on October 28, 2011. Data available from this CERES instrument is used in this study. CERES
climate data records involve an unprecedented level of data fusion: CERES measurements are combined with imager data (e.g., MODIS on Terra and Aqua, VIIRS on S-NPP), 4-D weather assimilation data, microwave sea-ice observations and measurements from five geostationary satellites to produce climate-quality radiative fluxes at the top-of-atmosphere, within the atmosphere and at the surface, together with the associated cloud and aerosol properties. CERES data has gone through extensive validation of both TOA and surface radiation using TOA consistency tests and direct comparisons of surface fluxes with ground-based measurements over both land and ocean. The TOA fluxes are a

factor of 2-3 better than Earth Radiation Budget Experiment (ERBE) and the flux record is highly stable. The CERES OLR datasets have a horizontal resolution (at nadir) of 20 Km. Suomi-NPP, CERES data (CER_ES8_NPP-FM5_Edition1-CV) for the period February 2014 to June 2019 is downloaded from earthdata.nasa.gov webpage. For the month of October, 2017, the data is not available on the said webpage.

Data selections criteria

To generate collocated dataset, INSAT-3D OLR was averaged for 3 × 3 pixels to match the CERES (about 20 km nadir) resolution and uniform scenes are used. The uniform scenes have small spatial variation and are measured by the coefficient of variation (CV) of INSAT-3D OLR. The CV is defined as the ratio of the standard deviation of INSAT-3D OLR to its mean value in 3 × 3 pixels for comparison with CERES. If the standard deviation of INSAT-3D OLR in 3 × 3 pixels is less than 1% of its mean value, the scene is judged to be uniform.

Finally, only those CERES observations which were obtained within ±5 minutes and 5 km radius of the INSAT-3D OLR were considered. Based on above criteria collocated points were obtained for each month. The validation is done over the region from 30° E to 130° E and 50° N to 40° S. The differences between the INSAT 3D OLR and NPP CERES OLR are calculated for each collocated point on monthly basis and are categorized in the range ±5 Wm^{-2} to ±20 Wm^{-2}. The statistical parameters are obtained for uniform scenes.

Chapter 3 Results & Discussion

3.1. Inter-comparison of INSAT-3D and CERES OLR

For comparing the satellite derived Outgoing longwave radiation from a geostationary platform and a polar platform, i.e., Imager payload onboard INSAT-3D satellite and CERES payload on Suomi NPP satellite, special care is taken while preparing collocated dataset. This is mainly because of the difference in spatial and temporal resolution of both the satellites. Hence as mentioned in above section, uniform scenes are used and collocated dataset is prepared subject to satisfying the above-mentioned data selection criteria.

3.1.1. 2D - Density plots

Fig. 5 shows the comparison, using density plots, between the CERES and INSAT-3D derived OLR products for the period February 2014 to June 2019 for each month. From the density plots it can be concluded that almost all points are lying on or below the line of unity referring to a very good correlation between INSAT-3D and CERES derived OLR products. It can be seen that INSAT-3D derived OLR is showing a negative bias (i.e., underestimation by INSAT-3D) throughout the study period. While interpreting the results it should be kept in mind that the OLR data available from INSAT-3D is at a better resolution then CERES derived OLR and it is averaged for collocation purpose. Hence, INSAT-3D derived OLR has a good potential for climatological purposes. To further assess the performance of INSAT-3D derived OLR statistical skill scores are also worked out.

4.1.2. **Statistical skill scores**

The collocated gridded comparison statistics are used to evaluate the performance of INSAT-3D OLR product.

For quantitative evaluation, following widely applied statistical metrices are used: Linear correlation coefficient (CC), Standard Deviation (SD), Bias, Root Mean Square deviation (RMSD), Bias Corrected Root Mean Square Deviation (URMSD). The statistical metrices are computed as follows:

$$\text{Bias} = \frac{1}{N}\sum_{i=1}^{N}(A)_i - (B)_i \quad (1)$$

$$\text{SD} = \sqrt{\left\{\frac{[N\sum_{i=1}^{N}(A_i-\overline{A})^2][N\sum_{i=1}^{N}(B_i-\overline{B})^2]}{N}\right\}} \quad (2)$$

$$\text{CC} = \frac{N(\sum_{i=1}^{N}A_iB_i)-(\sum_{i=1}^{N}A_i)(\sum_{i=1}^{N}B_i)}{\sqrt{[N\sum_{i=1}^{N}A^2{}_i-(\sum_{i=1}^{N}A_i)^2][N\sum_{i=1}^{N}B^2{}_i-(\sum_{i=1}^{N}B_i)^2]}} \quad (3)$$

$$\text{RMSD} = \sqrt{\frac{1}{N}\sum_{i=1}^{N}(A_i-B_i)^2} \quad (4)$$

$$\text{URMSD} = \sqrt{\text{RMSD}^2 - \text{BIAS}^2} \quad (5)$$

where, A is OLR derived using INSAT 3D, B is OLR derived using CERES and N is the number of samples.

Bias refers to the tendency of INSAT-3D derived OLR to over- or under-estimate with respect to that of CERES derived OLR. Standard Deviation tell us how the measurements of OLR from INSAT-3D are spread out from that of CERES. Correlation coefficient represents the linear relationship between two datasets. It lies between +1 to -1. RMSD is a measure of accuracy. Larger errors (i.e., deviations of INSAT-3D derived OLR from CERES OLR) will have a disproportionately large effect on RMSD.

The monthly correlation coefficient, bias and RMSD & URMSD variations for the period February, 2014 to June, 2019 is shown in Fig. 3(a), 3(b) & 3(c) respectively. The datasets exhibit a strong correlation throughout the period with a mean correlation of 0.94. It can be clearly seen from the Fig. 3(a) that, the quality of INSAT-3D derived OLR showed continuous degradation over the period with reaching a Minimum of 0.86 in April, 2016. However, after the application of GSICS correction in December, 2016, the quality of the product has shown improvement.

The collocated gridded comparison statistics (no. of collocated points, CC, Bias, RMSD, URMSD) for each month are shown in Table 5 and Fig. 3 respectively. It can be clearly seen from Table 5 that the Bias has increased from minimum bias of -1.42 Wm^{-2} in August, 2014 to -9.3 Wm^{-2} in November, 2016 which is maximum bias observed during the study period. The monthly bias maps at pixel level are also shown in Fig. 6 from June, 2014 to June, 2019. It can be seen from the bias maps that at sub-satellite point of INSAT-3D, it is under estimating consistently with a negative bias of -10 to -15 Wm^{-2}. However, this negative bias goes on decreasing when we move away from the sub-satellite point and changes to positive bias over landmass. Similarly, RMSD has also shown

increasing trend over the months from February, 2014 to November, 2016 with values in the range 8.6 to 14.15 Wm^{-2}.

To further investigate the quality of INSAT-3D OLR with respect to CERES OLR, the percentage of collocated points with biases ranging from -20 Wm-2 to 20 Wm^{-2} are calculated as shown in Fig. 4(a) and Table 6. The purpose of this segregation is to get a fair amount of idea of the nature and amount of biases which are dominating the overall bias as shown in Fig. 4(b) with number of collocated points on the extremes. It can be clearly seen from the figure that the number of collocated points between -5 Wm^{-2} to 5 Wm^{-2} were showing a declining trend whereas the number of collocated points less than -20 Wm^{-2} and greater than 20 Wm^{-2} were showing an increasing trend till December, 2016. This further points to importance of regular updating of radiance calibration coefficient values of INSAT-3D Imager in processing chain.

4.2. Impact of GSICS correction on the quality of INSAT-3D derived Outgoing longwave radiation

The INSAT-3D radiance coefficients were updated for the first time, in processing chain of INSAT-3D on 23rd December, 2016, at INSAT Meteorological Data Processing System (IMDPS), New Delhi, using GSICS correction carried out at Space application Centre, ISRO Ahmedabad. GSICS is an international collaborative effort initiated in 2005 by WMO and the CGMS to monitor, improve and harmonize the quality of observations from operational weather and environmental satellites of the Global Observing System (GOS). GSICS aims at ensuring consistent accuracy among space-based observations worldwide for climate monitoring, weather forecasting and environmental application (http://gsics.wmo.int/). It can be clearly seen from Fig. 3 and Fig. 5(b) that

after applying GSICS correction, the quality of INSAT-3D derived OLR has shown improvement. It can be clearly seen from the Figs. 3 & 6 and Table 5 that after implementation of GSICS correction, the Bias has come down from -7.54 Wm^{-2} in December 2016 to -2.81 Wm^{-2} in January 2017. The lowest bias observed after application of GSICS correction is -0.61 Wm^{-2} in July 2018. Similarly, RMSD came down from 11.39 Wm^{-2} in December 2016 to 8.62 Wm^{-2} in January 2017. The lowest RMSD observed after application of GSICS correction is 7.13Wm^{-2} in the month of May 2019. In terms of number of collocated points exhibiting biases, as shown in Figs. 4(a & b) and Table 6, it can be clearly seen that the number of collocated points between -5 Wm^{-2} to 5 Wm^{-2} increased from 22% in November 2016 to 53% in April 2017 and the number of collocated points having biases less than -20 Wm^{-2} and greater than 20 Wm^{-2} decreased from 7% in November 2016 to 2.5% in January 2017.

Chapter 5 Summary and conclusions

This study evaluated the performance of INSAT-3D derived Outgoing Longwave Radiation, generated from operational IMDPS, New Delhi with Suomi-NPP, CERES derived Outgoing Longwave Radiation product over the domain from 30° E to 130° E and 50° N to 40° S during July 2014 to June 2019. For the uniform scenes, the bias between CERES and INSAT-3D OLR lies in the range of -1.42 to -9.3 Wm-2, the correlation coefficient lies in the range 0.86 to 0.97 and RMSD lies in the range of 8.11 to 12.21 Wm-2. The validation results suggest that the OLR estimated using INSAT-3D Imager radiance is of good quality (with mean CC 0.92, bias -5.32 Wm-2, RMSD 10.31 Wm-2 & URMSD 8.58 Wm-2). To facilitate comparison between the INSAT 3D OLR and CERES OLR, the INSAT-3D OLR was averaged over 3 × 3 pixels which otherwise offers a better resolution at 8 km per pixel at nadir. After applying GSICS correction in INSAT-3D radiance coefficient, the quality of INSAT-3D derived OLR has shown improvement. Therefore, it is suggested that the GSICS correction need to be applied at regular intervals to maintain the accuracy and quality of product. Considering the quality of INSAT-3D OLR which closely matches with CERES and the higher spatial as well as temporal resolution of INSAT-3D OLR and CERES OLR suggest that the INSAT-3D derived OLR could be used in the various applications and climatological studies.

Refrences:

1. Ba, M. B., Ellingson, R. G. and Gruber, A., 2003, “Validation of a technique for estimating OLR with the GOES sounder”, Journal of atmospheric and oceanic technology, 20, 1, 79-89.
2. Cheruy, F., Kandel, R. S. and Duvel, J. P., 1991, “Outgoing longwave radiation and its diurnal variation from combined ERBE and Meteosat observations: 1. Estimating OLR from Meteosat data. Journal of Geophysical Research: Atmospheres, 96, D12, 22611-22622.
3. Ellingson, R. G. and Ferrado, R. R., 1983, “An examination of a technique for estimating the longwave radiation budget from satellite radiance observations”, Journal of climate and applied meteorology, 22, 8, 1416-1423.
4. Ellingson, R. G., Lee, H. T., Yanuk, D. and Gruber, A., 1994, “Validation of a technique for estimating outgoing longwave radiation from HIRS radiance observations’, journal of atmospheric and oceanic technology, 11, 2, 357-365.
5. Ellingson, R. G., Yanuk, D. J., Lee, H. T. and Gruber, A., 1989, “A technique for estimating outgoing longwave radiation from HIRS radiance observations”, Journal of atmospheric and oceanic technology, 6, 4, 706-711.
6. Gruber, A., and Krueger, A. F., 1984, “The status of the NOAA outgoing longwave radiation data set”, Bulletin of the American Meteorological Society, 65, 9, 958-962.
7. Gruber, A., and Winston, J. S., 1978, ‘Earth-atmosphere radiative heating based on NOAA scanning radiometer measurements”, Bulletin of the American Meteorological Society, 59, 12, 1570-1573.
8. Gruber, A., Ellingson, R. G., Ardanuy, P., Weiss, M., Yang, S. K. and Oh, S. N., 1994, “A comparison of ERBE and AVHRR longwave flux estimates”, Bulletin of the American meteorological society, 75, 11, 2115-2130.
9. Lee, H. T., Gruber, A., Ellingson, R. G. And Laszlo, I., 2007, “Development of the HIRS outgoing longwave radiation climate dataset”, Journal of atmospheric and oceanic technology, 24, 12, 2029-2047.
10. Lee, H. T., Heidinger, A., Gruber, A. and Ellingson, R. G., 2004, “The HIRS outgoing longwave radiation product from hybrid polar and geosynchronous satellite observations”, Advances in Space Research, 33, 7, 1120-1124.
11. Minnis, P., Young, D. F. and Harrison, E. F., 1991, “Examination of the relationship between outgoing infrared window and total longwave fluxes using satellite data”, Journal of climate, 4, 11, 1114-1133.

12. Schmetz, J. and Liu, Q., 1988, “Outgoing longwave radiation and its diurnal variation at regional scales derived from Meteosat”, Journal of geophysical research: atmospheres, 93, D9, 11192-11204.
13. Singh, R., Ojha, S. P., Kishtawal, C. M., Pal, P. K. and Kiran Kumar, A. S., 2015, “Impact of the assimilation of INSAT-3D radiances on short-range weather forecasts”, Q. J. R. Meteorol. Soc., 142, 694, 120-131, doi:10.1002/qj.2636.
14. Singh, R., Singh, C., Ojha, S. P., Kumar, A. S., Kishtawal, C. M. and Kiran Kumar, A. S., 2016, “Land surface temperature from INSAT-3D imager data: Retrieval and assimilation in NWP model”, J. Geophys. Res. Atmos., 121, 12, 6906-6926, doi:10.1002/2016JD024752.
15. Singh, R., Thapliyal, P. K., Kishtawal, C. M. and Pal, P. K., “Outgoing Longwave Radiation Product ATBD”, DOI:10.19038/SAC/10/3DIMG_L2B_OLR.
16. Singh, R., Thapliyal, P. K., Kishtawal, C. M., Pal, P. K. and Joshi, P. C., 2007, “A new technique for estimating outgoing longwave radiation using infrared window and water vapor radiances from Kalpana very high resolution radiometer”, Geophysical Research Letters, 34, 23, L23815, doi:10.1029/2007GL031715.

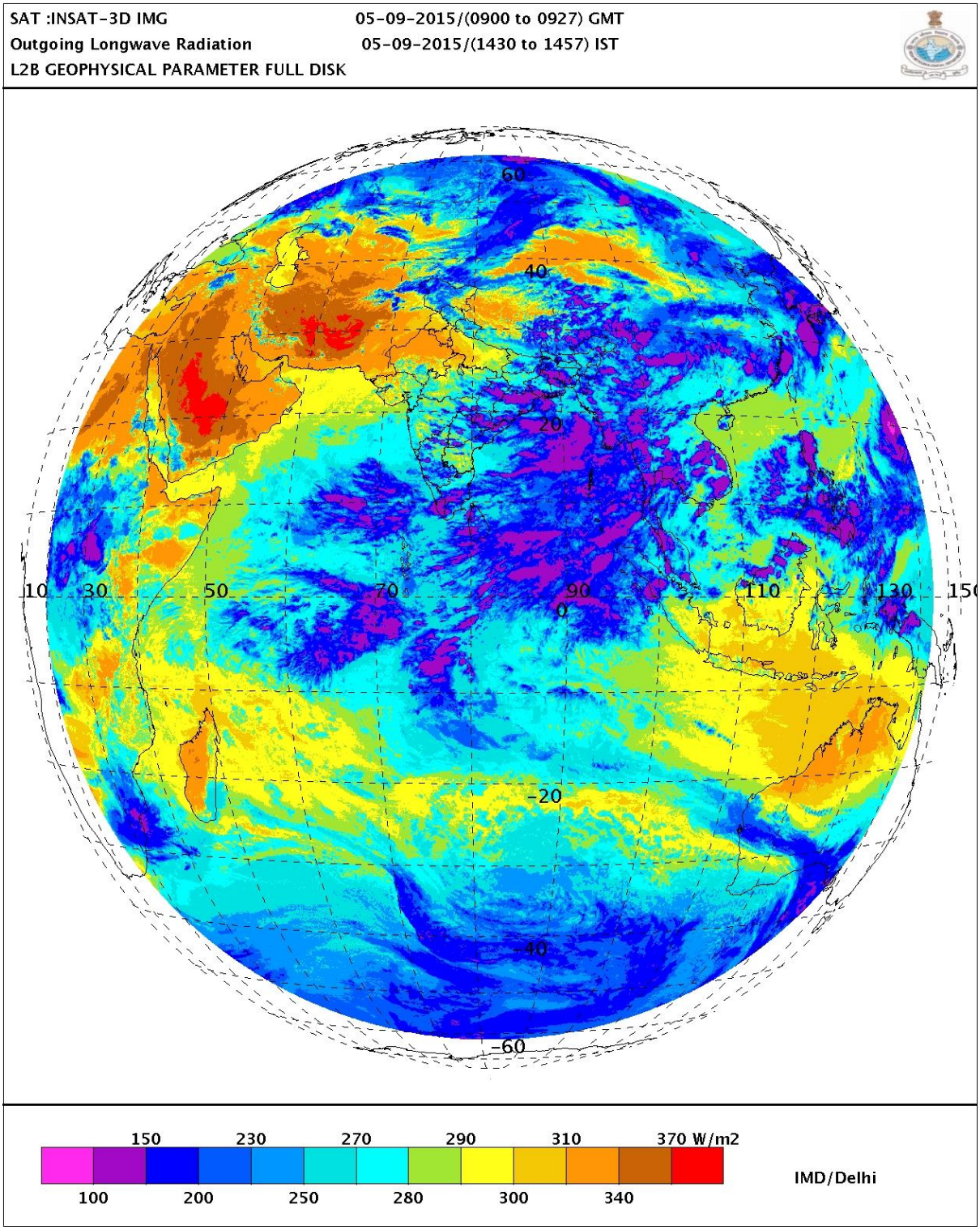

Fig. 1. INSAT-3D OLR (Wm^{-2}) 0900UTC of 05th September, 2016

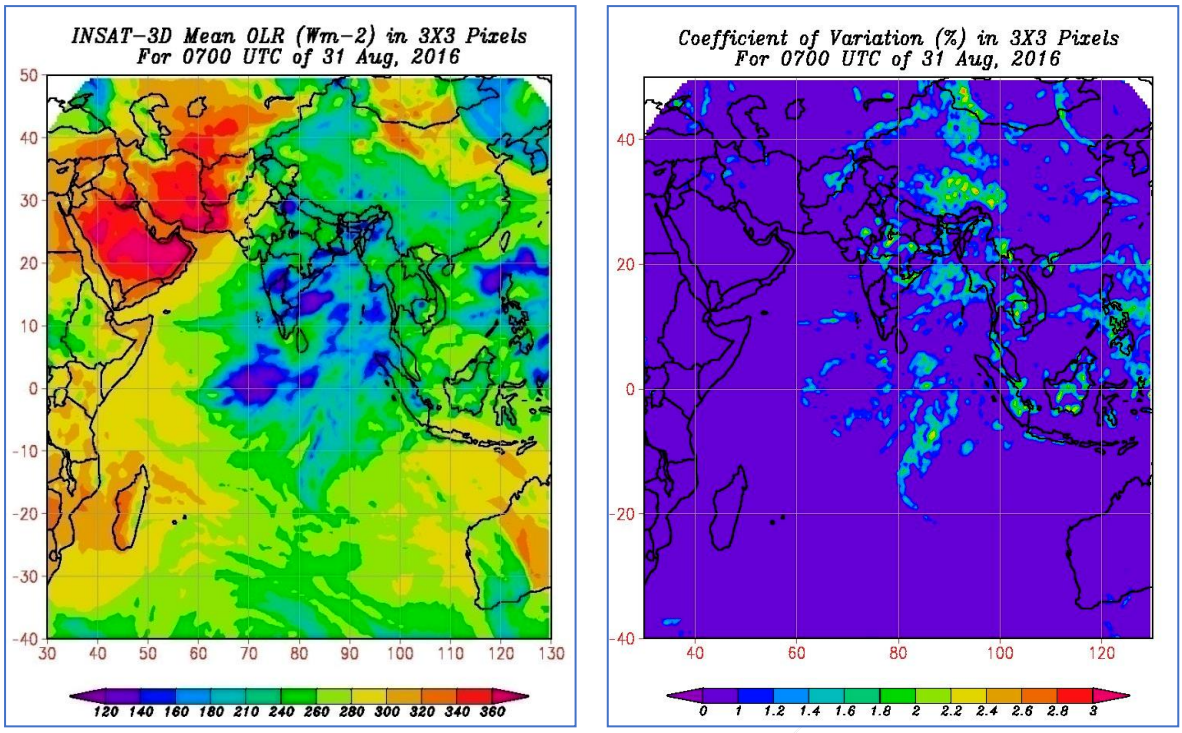

Fig. 2. INSAT-3D mean OLR (Wm^{-2}) in 3 × 3 pixels (upper panel) and coefficient of variation (%) in 3 × 3 pixels (lower panel), 0700 UTC 31 August, 2016

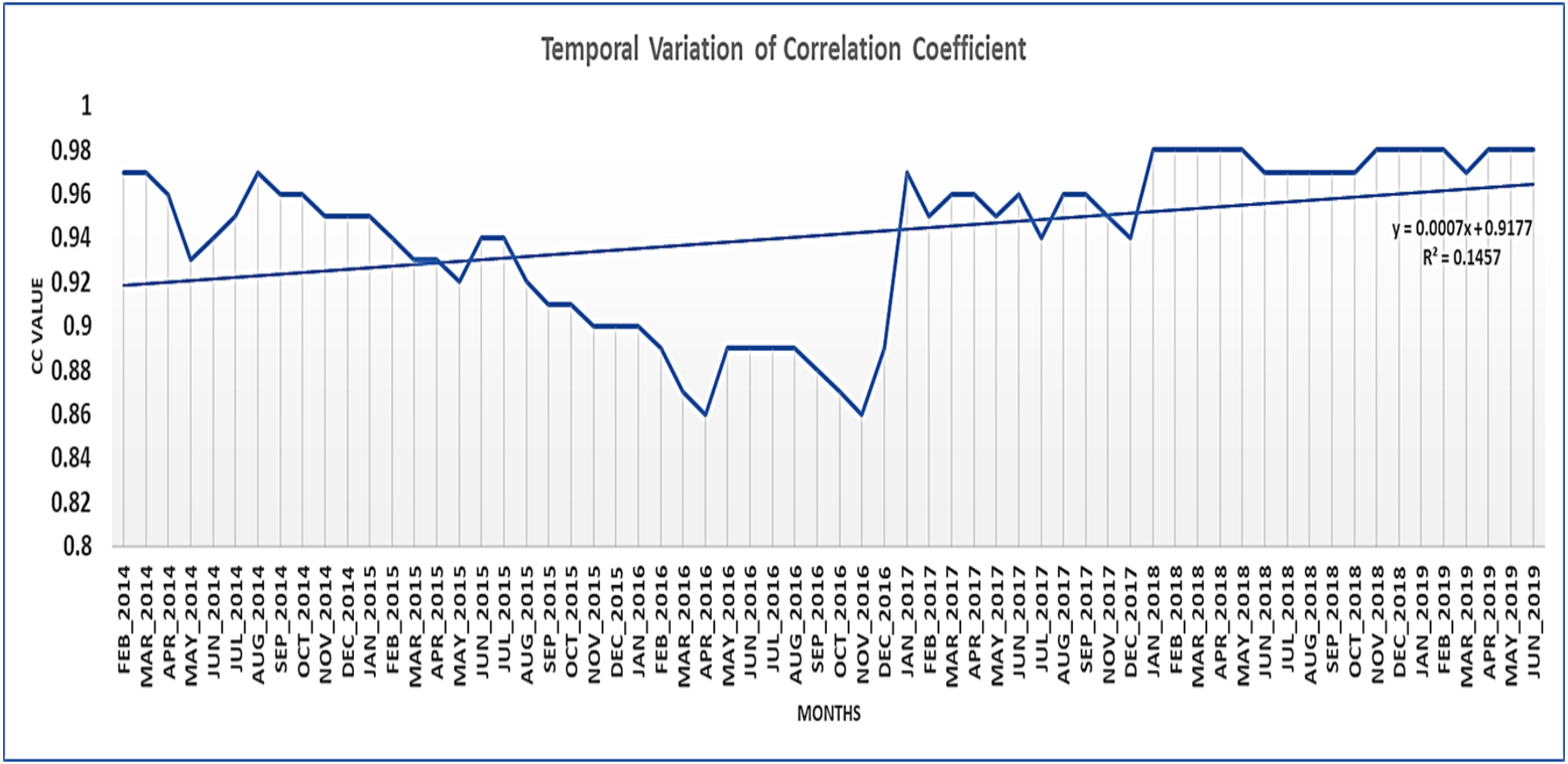

Fig 3(a): Monthly correlation of INSAT-3D OLR with CERES from February 2014 to June 2019

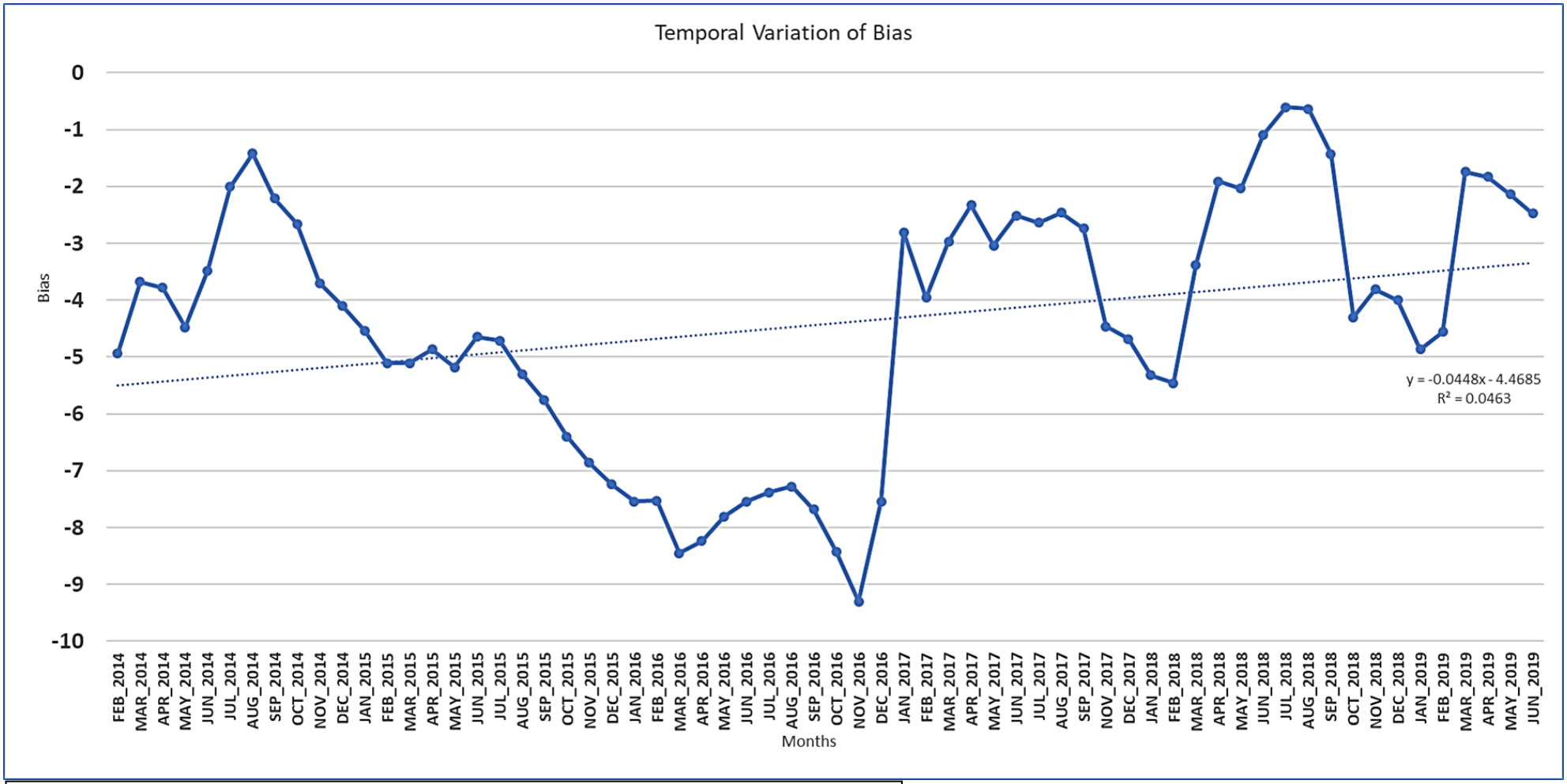

Fig 3(b): Monthly bias of INSAT-3D OLR with CERES from February 2014 to June 2019

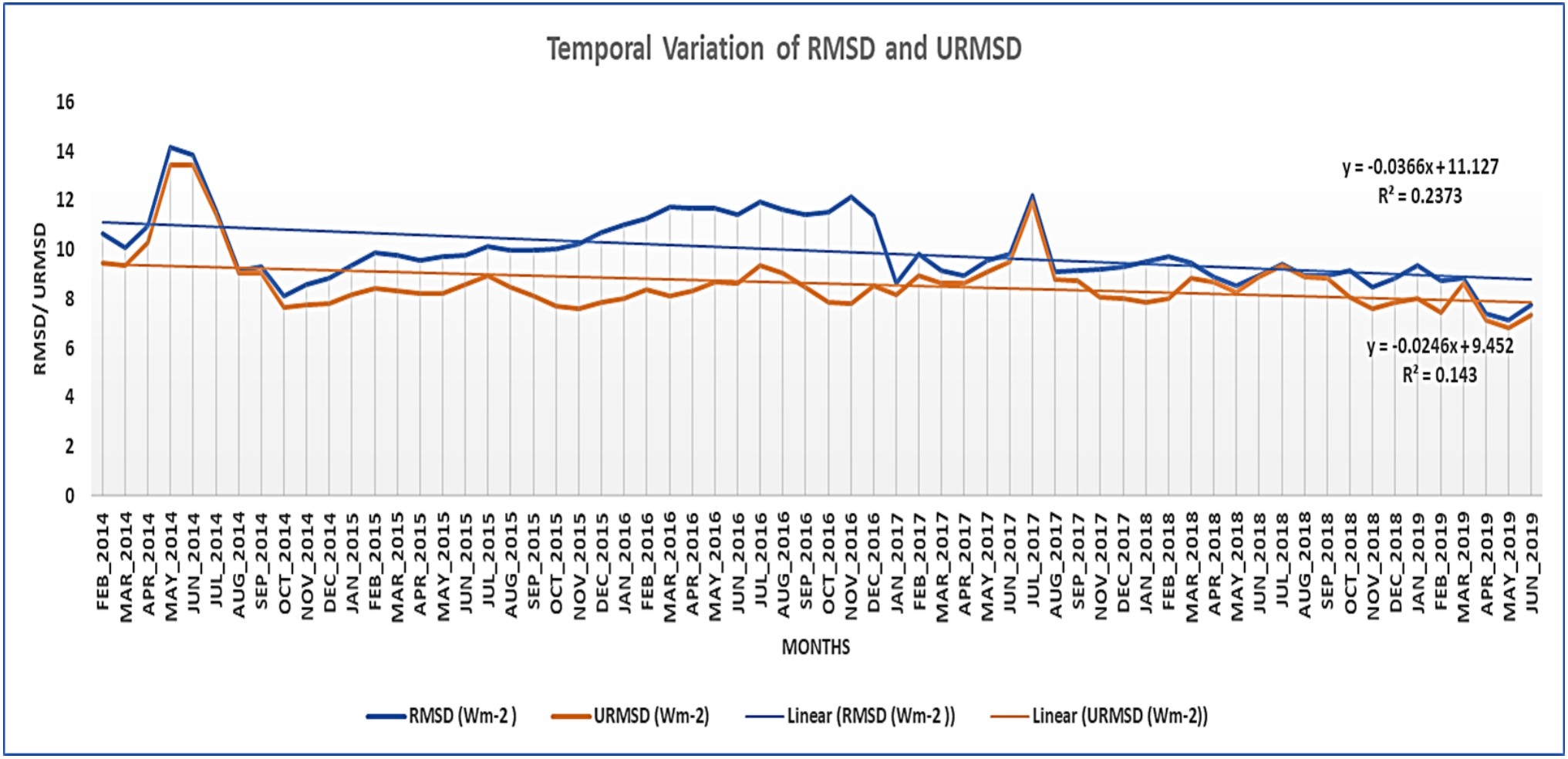

Fig 3(c): Monthly RMSD & URMSD of INSAT-3D OLR with CERES from February 2014 to June 2019

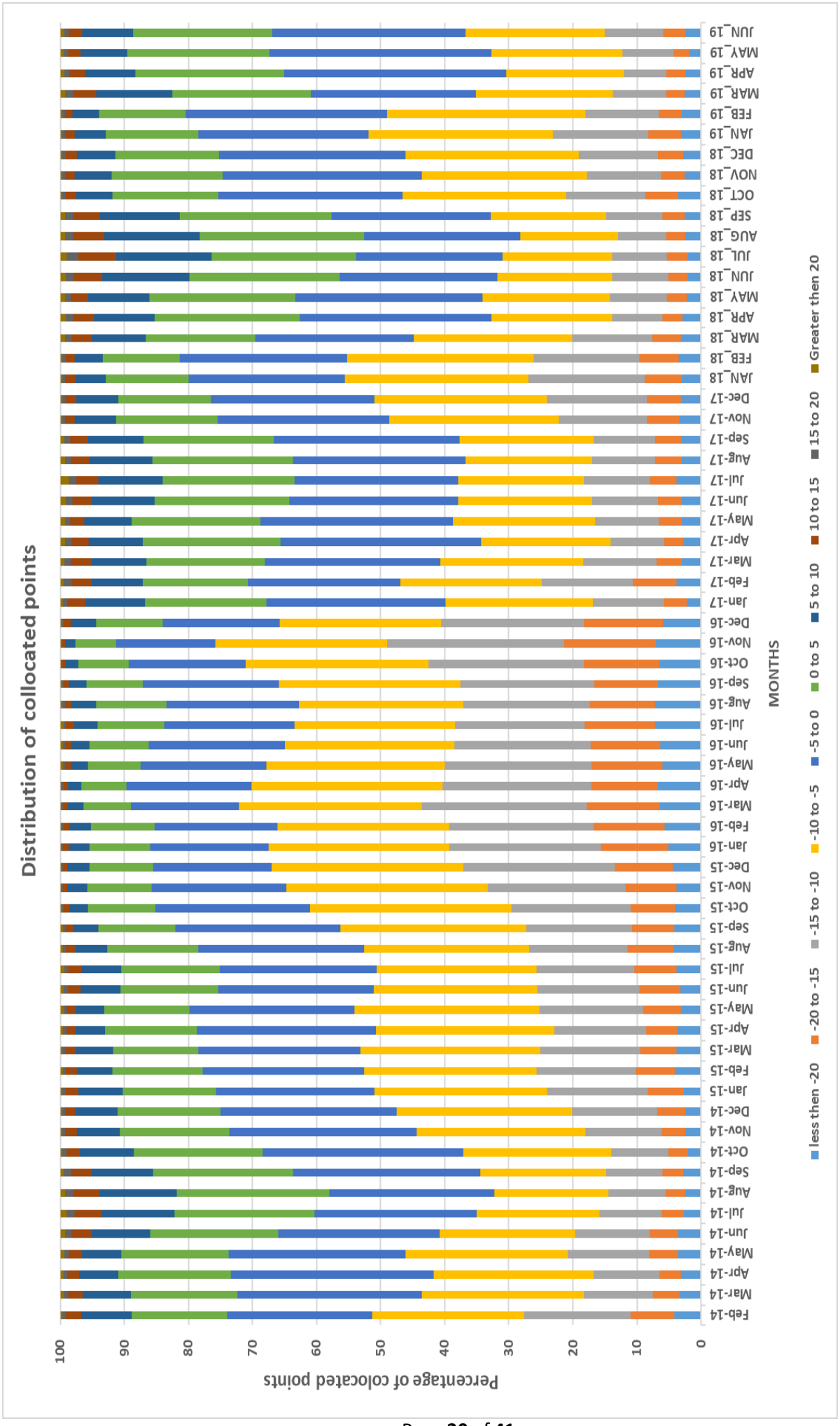

Fig 4(a): The percentage of collocated points with respect to bias

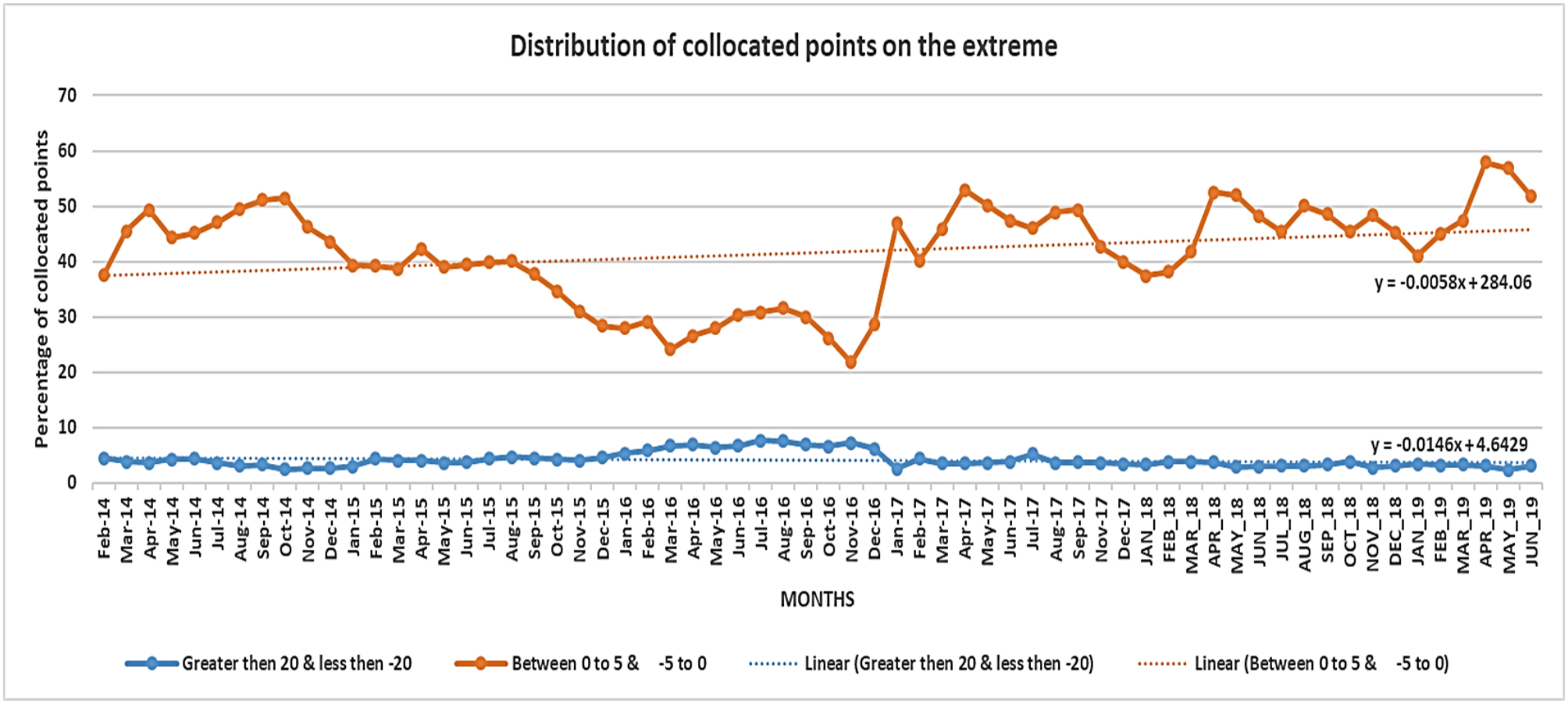

Fig 4(b): The percentage of collocated points on the extremes with respect to bias

Month	Collocated Points	Correlation Coefficient	Bias (Wm-2)	RMSD (Wm-2)	URMSD (Wm-2)	Mean INSAT-3D OLR	Mean CERES OLR
FEB_2014	105559	0.97	-4.94	10.66	9.44	265.53	270.46
MAR_2014	97225	0.97	-3.68	10.06	9.37	271.94	275.62
APR_2014	84122	0.96	-3.78	10.96	10.29	276.9	280.68
MAY_2014	102081	0.93	-4.48	14.15	13.42	272.37	276.85
JUN_2014	112906	0.94	-3.48	13.86	13.42	275.17	278.65
JUL_2014	126337	0.95	-2.01	11.6	11.43	272.63	274.64
AUG_2014	102467	0.97	-1.42	9.16	9.05	276.8	278.22
SEP_2014	85826	0.96	-2.21	9.29	9.03	279.2	281.41
OCT_2014	107902	0.96	-2.66	8.11	7.67	274.16	276.82
NOV_2014	114748	0.95	-3.7	8.6	7.76	265.09	268.79
DEC_2014	129168	0.95	-4.1	8.84	7.83	262.88	266.98
JAN_2015	137500	0.95	-4.54	9.36	8.19	265.28	269.82
FEB_2015	103891	0.94	-5.11	9.86	8.44	267.73	272.84
MAR_2015	103333	0.93	-5.11	9.75	8.3	271.27	276.39
APR_2015	82078	0.93	-4.87	9.57	8.24	274.11	278.99
MAY_2015	114901	0.92	-5.18	9.7	8.2	272.33	277.51
JUN_2015	122422	0.94	-4.65	9.78	8.6	271.7	276.35
JUL_2015	134897	0.94	-4.71	10.12	8.96	272.85	277.56
AUG_2015	103272	0.92	-5.3	9.98	8.46	276.32	281.61
SEP_2015	93794	0.91	-5.76	9.96	8.12	276.25	282
OCT_2015	98792	0.91	-6.4	10.01	7.71	271.2	277.59
NOV_2015	117251	0.9	-6.86	10.25	7.62	264.55	271.4
DEC_2015	134460	0.9	-7.24	10.68	7.85	261.25	268.49
JAN_2016	136500	0.9	-7.54	11.01	8.02	259.34	266.89
FEB_2016	110936	0.89	-7.53	11.28	8.39	266.66	274.2
MAR_2016	102756	0.87	-8.45	11.73	8.13	269.27	277.72
APR_2016	81595	0.86	-8.24	11.71	8.32	272.22	280.46
MAY_2016	105478	0.89	-7.81	11.67	8.67	269.36	277.17
JUN_2016	118761	0.89	-7.54	11.45	8.61	266.47	274.01
JUL_2016	118691	0.89	-7.38	11.93	9.38	265.85	273.22
AUG_2016	95540	0.89	-7.28	11.63	9.07	271.59	278.87
SEP_2016	90094	0.88	-7.68	11.43	8.46	274.25	281.93
OCT_2016	84137	0.87	-8.42	11.53	7.88	270.04	278.47
NOV_2016	119860	0.86	-9.3	12.14	7.81	262.87	272.16
DEC_2016	135405	0.89	-7.54	11.39	8.54	263.92	271.46
JAN_2017	134388	0.97	-2.81	8.62	8.15	266.52	269.32
FEB_2017	105488	0.95	-3.96	9.8	8.97	268.06	272.02
MAR_2017	96495	0.96	-2.97	9.15	8.66	272.85	275.82
APR_2017	84428	0.96	-2.33	8.95	8.64	280.11	282.43
MAY_2017	104115	0.95	-3.04	9.59	9.1	275.67	278.7
JUN_2017	110112	0.96	-2.51	9.82	9.49	274.5	277.01
JUL_2017	120680	0.94	-2.64	12.21	11.92	272.01	274.66
AUG_2017	94478	0.96	-2.46	9.11	8.77	276.65	279.11
SEP_2017	89723	0.96	-2.74	9.15	8.73	278.85	281.59
NOV_2017	116328	0.95	-4.46	9.21	8.06	266.37	270.82
DEC_2017	128313	0.94	-4.68	9.3	8.04	264.42	269.11
JAN_2018	50258	0.98	-5.32	9.5	7.88	262.33	267.65
FEB_2018	101397	0.98	-5.46	9.7	8.02	265.39	270.85
MAR_2018	98758	0.98	-3.38	9.48	8.86	275.01	278.4
APR_2018	78414	0.98	-1.91	8.88	8.67	276.69	278.6
MAY_2018	106026	0.98	-2.04	8.53	8.28	274.42	276.46
JUN_2018	121366	0.97	-1.09	8.93	8.87	275.14	276.22
JUL_2018	118620	0.97	-0.61	9.39	9.37	275.38	275.99

AUG_2018	100663	0.97	-0.64	8.92	8.9	279.94	280.57
SEP_2018	87593	0.97	-1.43	8.94	8.82	281.41	282.83
OCT_2018	108135	0.97	-4.3	9.13	8.06	272.72	277.03
NOV_2018	121532	0.98	-3.81	8.48	7.58	267.58	271.39
DEC_2018	134462	0.98	-4	8.82	7.86	263.33	267.33
JAN_2019	124076	0.98	-4.87	9.36	8	264.42	269.29
FEB_2019	109585	0.98	-4.56	8.74	7.46	269.42	273.99
MAR_2019	88911	0.97	-1.74	8.84	8.66	275.69	277.43
APR_2019	82116	0.98	-1.83	7.37	7.14	278.73	280.56
MAY_2019	116743	0.98	-2.14	7.13	6.81	277.06	279.2
JUN_2019	118548	0.98	-2.48	7.74	7.34	271.48	273.96

Table5: The collocated gridded comparison statistics (no. of collocated points, CC, Bias, RMSD, URMSD) for each month from February 2014 to June 2019.

Month	Percentage of collocated points from INSAT-3D w.r.t. CERES in terms of Bias (Wm-2)											
	less then -20	-20 to -15	-15 to -10	-10 to -5	-5 to 0	0 to 5	5 to 10	10 to 15	15 to 20	Greater then 20	Greater then 20 & less then -20	Between 0 to 5 & -5 to 0
Feb-14	4.18	6.78	16.62	23.79	22.54	15.01	7.76	2.43	0.61	0.27	4.45	37.55
Mar-14	3.34	4.15	10.83	25.2	28.81	16.68	7.46	2.37	0.69	0.47	3.81	45.49
Apr-14	3.12	3.4	10.23	24.94	31.65	17.64	6.07	1.82	0.65	0.48	3.6	49.29
May-14	3.65	4.43	12.72	25.29	27.61	16.76	6.14	2.05	0.73	0.62	4.27	44.37
Jun-14	3.64	4.36	11.71	21.08	25.22	19.92	9.24	3.11	0.98	0.76	4.4	45.14
Jul-14	2.66	3.44	9.78	19.2	25.26	21.81	11.43	4.17	1.32	0.92	3.58	47.07
Aug-14	2.39	3.17	8.87	17.81	25.74	23.8	12.1	4.13	1.24	0.73	3.12	49.54
Sep-14	2.81	3.19	8.81	19.58	29.28	21.84	9.66	3.23	1.06	0.55	3.36	51.12
Oct-14	2.1	2.96	8.91	23.18	31.22	20.21	8.39	2.11	0.6	0.32	2.42	51.43
Nov-14	2.38	3.8	11.87	26.33	29.22	17.07	6.8	1.75	0.5	0.28	2.66	46.29
Dec-14	2.45	4.33	13.39	27.36	27.45	16.12	6.5	1.65	0.47	0.27	2.72	43.57
Jan-15	2.66	5.62	15.75	26.9	24.72	14.6	6.93	1.99	0.52	0.3	2.96	39.32
Feb-15	4.05	6.1	15.49	26.97	25.17	14.07	5.59	1.71	0.52	0.32	4.37	39.24
Mar-15	3.82	5.71	15.6	28	25.32	13.34	5.87	1.59	0.47	0.28	4.1	38.66
Apr-15	3.69	4.82	14.34	27.86	28.05	14.3	4.56	1.41	0.56	0.41	4.1	42.35
May-15	3.15	5.89	16.13	28.95	25.69	13.33	4.49	1.42	0.5	0.44	3.59	39.02
Jun-15	3.22	6.36	15.92	25.61	24.29	15.16	6.26	1.94	0.72	0.51	3.73	39.45
Jul-15	3.81	6.57	15.32	24.93	24.46	15.45	6.22	2.02	0.64	0.59	4.4	39.91
Aug-15	4.32	7.12	15.42	25.73	25.84	14.26	5.02	1.43	0.49	0.36	4.68	40.1
Sep-15	4.21	6.49	16.63	29.01	25.69	12.01	3.96	1.25	0.42	0.32	4.53	37.7
Oct-15	4.05	6.99	18.53	31.41	24.17	10.51	2.96	0.87	0.28	0.22	4.27	34.68
Nov-15	3.88	7.95	21.49	31.45	21	10.09	3.01	0.72	0.24	0.16	4.04	31.09
Dec-15	4.41	8.95	23.73	29.99	18.49	9.92	3.38	0.75	0.22	0.16	4.57	28.41
Jan-16	5.12	10.47	23.68	28.28	18.46	9.47	3.2	0.9	0.25	0.17	5.29	27.93
Feb-16	5.67	11.09	22.57	26.8	19.16	9.93	3.36	0.96	0.28	0.19	5.86	29.09
Mar-16	6.49	11.36	25.68	28.63	16.84	7.34	2.55	0.68	0.25	0.18	6.67	24.18
Apr-16	6.68	10.43	23.28	29.74	19.51	7.07	2.09	0.75	0.25	0.21	6.89	26.58
May-16	6.01	11.07	22.93	27.78	19.65	8.27	2.65	0.91	0.4	0.33	6.34	27.92
Jun-16	6.37	10.85	21.29	26.48	21.26	9.19	2.93	0.9	0.37	0.35	6.72	30.45
Jul-16	7.21	10.9	20.29	25.01	20.41	10.39	3.69	1.22	0.42	0.48	7.69	30.8
Aug-16	7.2	10.12	19.75	25.74	20.68	10.9	3.85	1.05	0.4	0.32	7.52	31.58
Sep-16	6.67	10	20.87	28.37	21.27	8.7	2.8	0.85	0.26	0.21	6.88	29.97
Oct-16	6.5	11.72	24.36	28.5	18.26	7.88	2.01	0.48	0.17	0.11	6.61	26.14
Nov-16	7.08	14.35	27.53	26.8	15.57	6.28	1.68	0.43	0.15	0.13	7.21	21.85
Dec-16	5.91	12.34	22.37	25.18	18.24	10.33	4.01	1.07	0.33	0.22	6.13	28.57
Jan-17	2.17	3.62	11.09	23.02	27.96	18.96	9.26	2.82	0.72	0.38	2.55	46.92
Feb-17	3.8	6.84	14.27	22.06	23.76	16.44	7.9	3.16	1.22	0.57	4.37	40.2
Mar-17	2.96	3.94	11.5	22.26	27.44	18.45	8.56	3.24	1.09	0.55	3.51	45.89
Apr-17	2.83	2.99	8.29	20.19	31.37	21.52	8.34	2.69	1.07	0.7	3.53	52.89
May-17	2.97	3.59	9.95	22.2	30.07	20.12	7.32	2.29	0.8	0.68	3.65	50.19
Jun-17	2.99	3.67	10.33	20.93	26.3	21.07	9.83	3.03	1.01	0.84	3.83	47.37
Jul-17	3.87	4.15	10.2	19.73	25.53	20.52	10.13	3.36	1.18	1.34	5.21	46.05
Aug-17	3	4.17	9.84	19.78	26.93	21.95	9.78	2.87	1.01	0.67	3.67	48.88
Sep-17	3.17	4.06	9.55	20.92	29.03	20.25	8.7	2.81	0.88	0.61	3.78	49.28
Nov-17	3.33	5.11	13.78	26.4	26.83	15.83	6.46	1.55	0.46	0.25	3.58	42.66
Dec-17	3.17	5.32	15.51	26.97	25.59	14.43	6.6	1.68	0.46	0.26	3.43	40.02
JAN_18	3	5.83	18.07	28.67	24.39	13	4.75	1.51	0.49	0.3	3.3	37.39
FEB_18	3.5	6.1	16.48	29.18	26.1	12.04	4.32	1.45	0.53	0.31	3.81	38.14

MAR_18	3.16	4.48	12.42	24.75	24.72	17.11	8.52	3.11	1.06	0.68	3.84	41.83
APR_18	2.91	3.1	7.86	18.88	29.84	22.65	9.53	3.22	1.2	0.81	3.72	52.49
MAY_18	2.18	3.17	8.92	19.87	29.14	22.87	9.51	2.72	0.88	0.73	2.91	52.01
JUN_18	2.14	2.97	8.71	17.94	24.68	23.43	13.59	4.42	1.31	0.81	2.95	48.11
JUL_18	2.14	3.15	8.59	17.11	22.9	22.46	14.97	5.89	1.8	1	3.14	45.36
AUG_18	2.41	2.98	7.6	15.17	24.41	25.66	14.95	4.84	1.31	0.68	3.09	50.07
SEP_18	2.54	3.45	8.85	17.98	24.82	23.77	12.47	4.12	1.28	0.72	3.26	48.59
OCT_18	3.54	5.09	12.44	25.49	28.85	16.51	5.59	1.63	0.54	0.32	3.86	45.36
NOV_18	2.52	3.73	11.6	25.77	31.06	17.29	5.83	1.52	0.44	0.23	2.75	48.35
DEC_18	2.74	4.03	12.31	26.99	29.11	16.19	6.01	1.74	0.57	0.32	3.06	45.3
JAN_19	3.12	5.06	14.92	28.76	26.64	14.36	4.94	1.46	0.47	0.29	3.41	41
FEB_19	2.99	3.62	11.37	31	31.41	13.59	4.1	1.25	0.41	0.26	3.25	45
MAR_19	2.58	2.9	8.25	21.38	25.76	21.68	11.84	3.65	1.26	0.69	3.27	47.44
APR_19	2.47	2.99	6.57	18.4	34.61	23.27	7.82	2.42	0.8	0.65	3.12	57.88
MAY_19	1.83	2.51	7.93	20.43	34.64	22.28	7.25	1.9	0.7	0.53	2.36	56.92
JUN_19	2.49	3.39	9.12	21.77	30.11	21.79	7.91	2.08	0.74	0.61	3.1	51.9

Table 6: Percentage of collocated points from INSAT-3D w.r.t. CERES in terms of Bias (Wm-2)

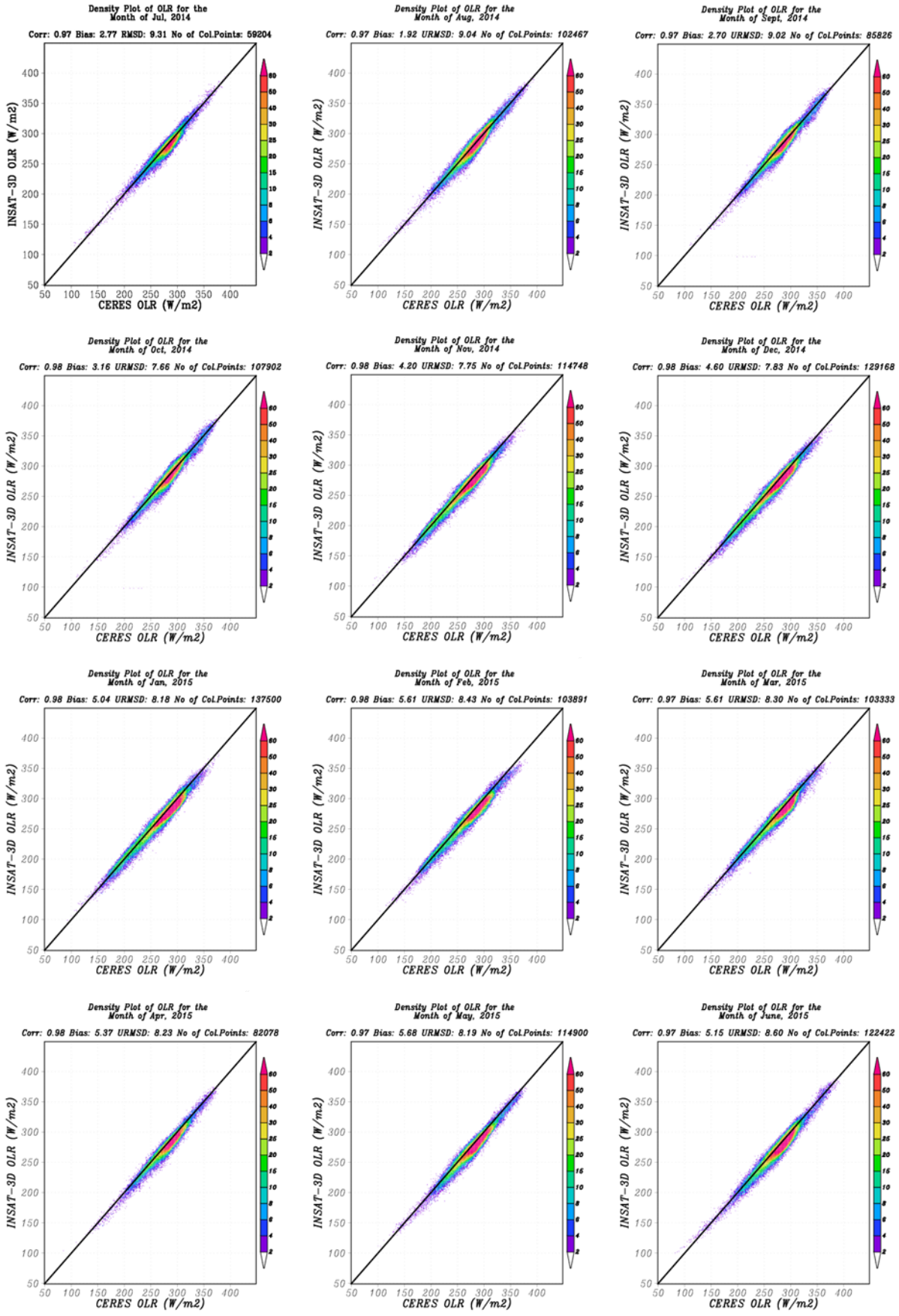

Fig 5: Density Plots between INSAT-3D, Imager OLR and Suomi-NPP, CERES OLR (June 2014 to June 2015)

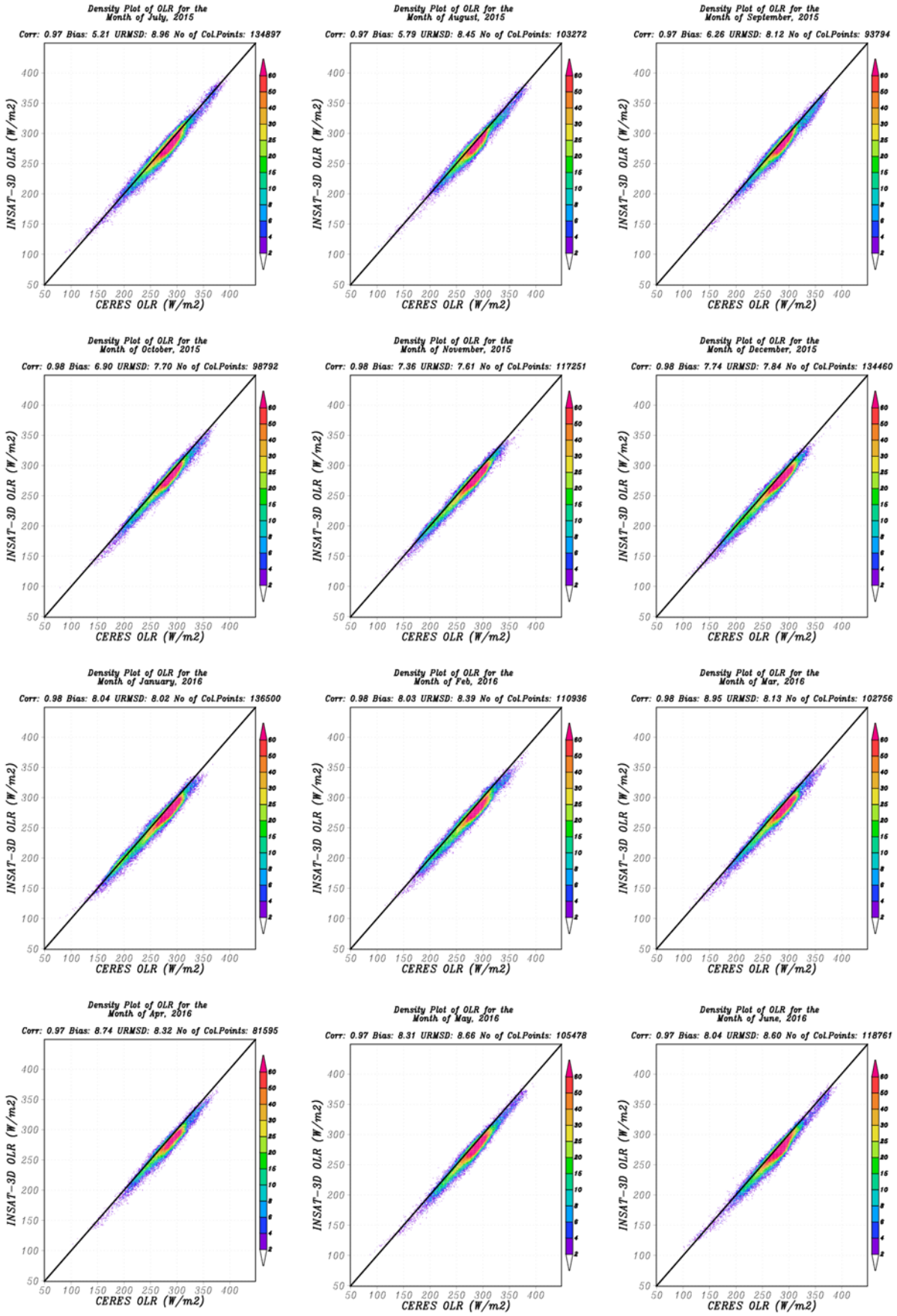

Fig 5: Density Plots between INSAT-3D, Imager OLR and Suomi-NPP, CERES OLR (July 2015 to June 2016)

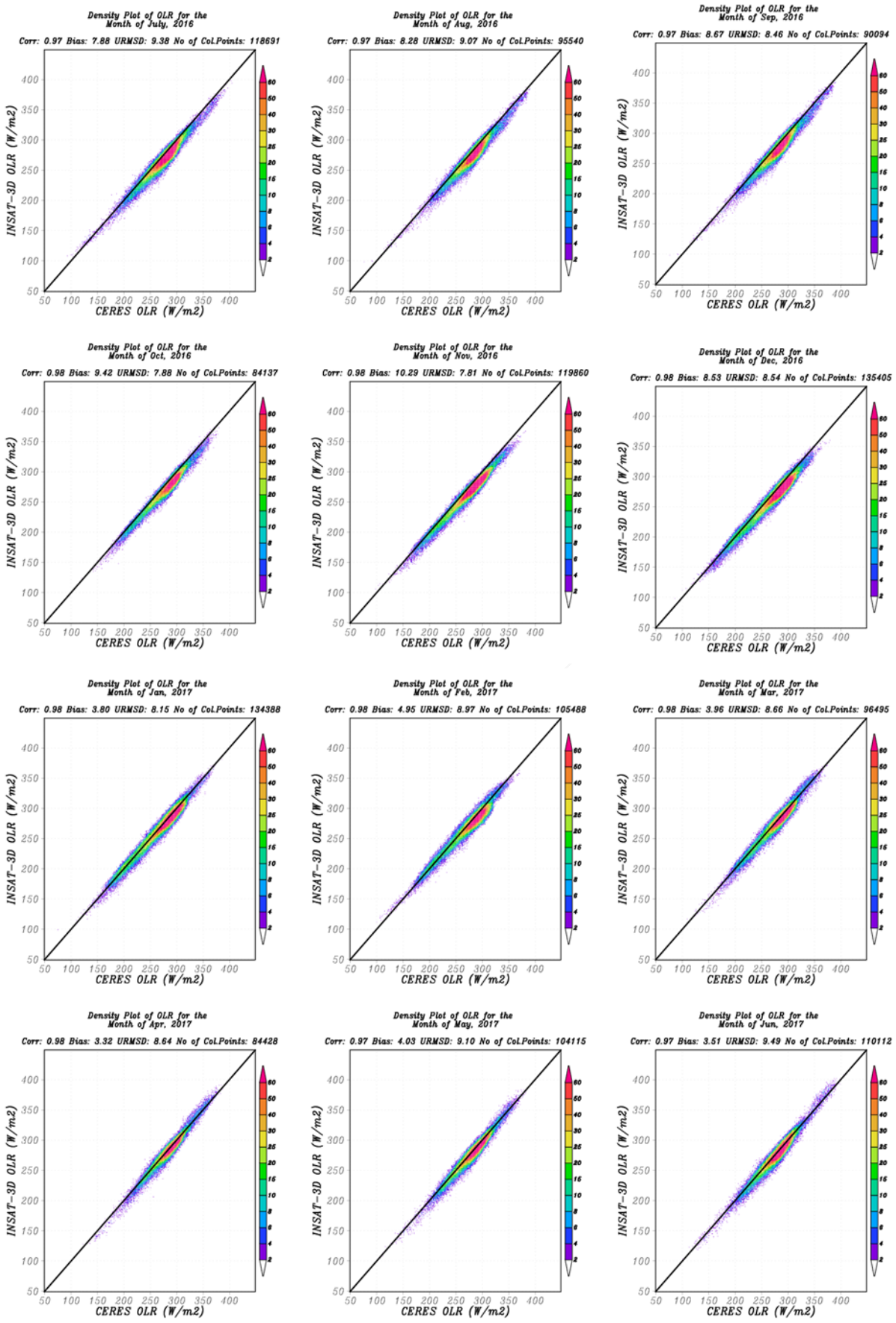

Fig 5: Density Plots between INSAT-3D, Imager OLR and Suomi-NPP, CERES OLR (July 2016 to June 2017)

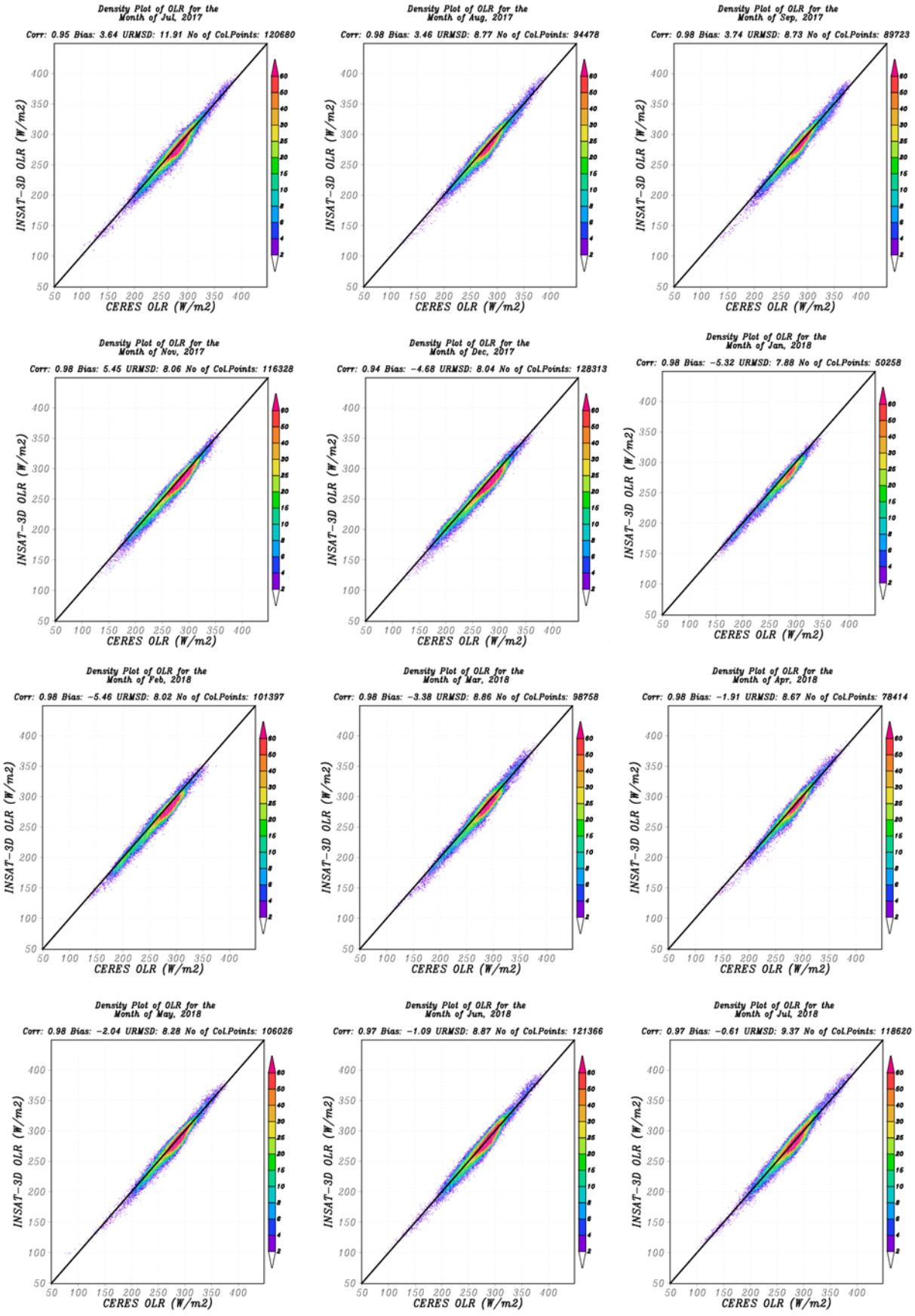

Fig 5: Density Plots between INSAT-3D, Imager OLR and Suomi-NPP, CERES OLR (July 2017 to July 2018)

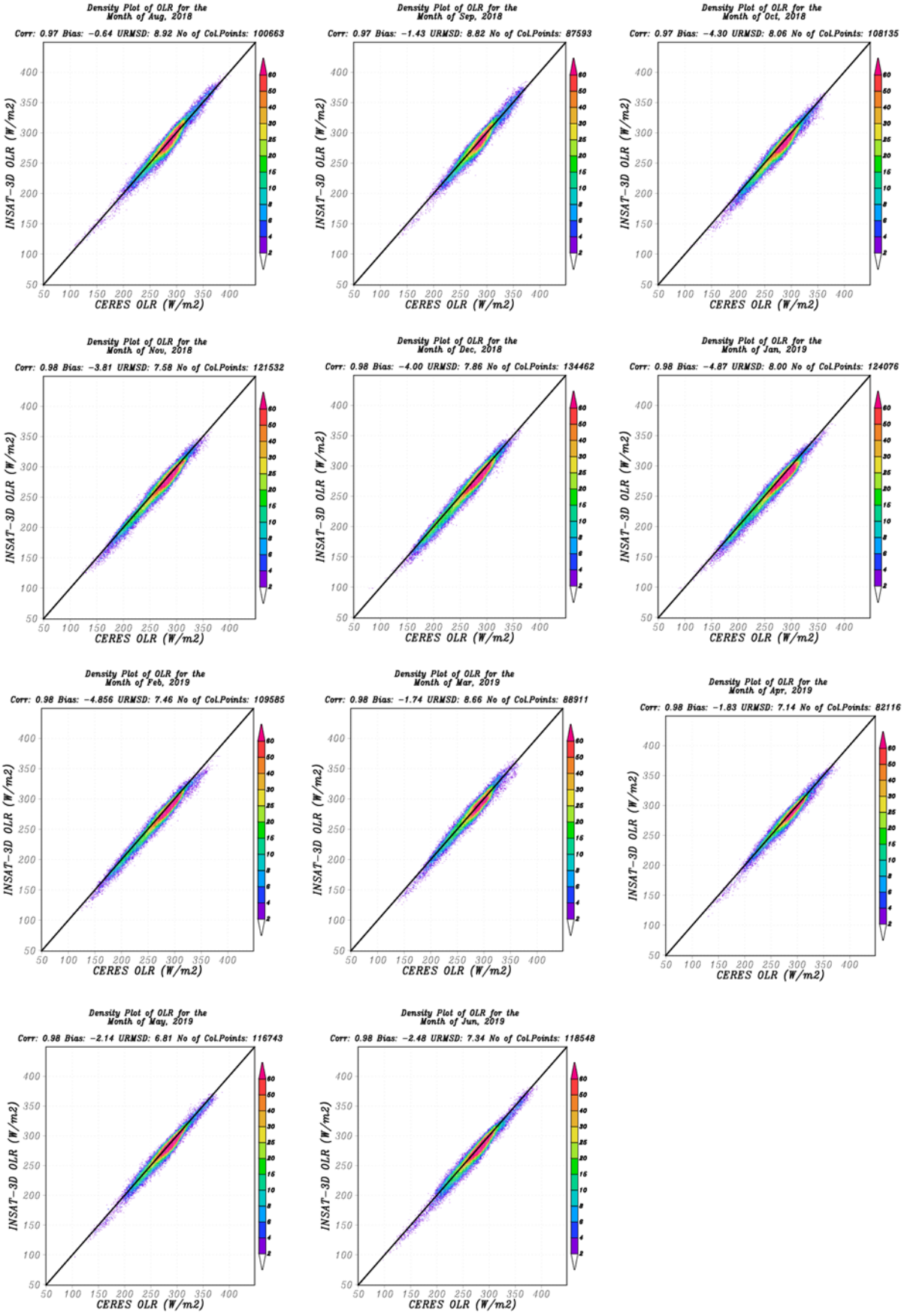

Fig 5: Density Plots between INSAT-3D, Imager OLR and Suomi-NPP, CERES OLR (August 2018 to June 2019)

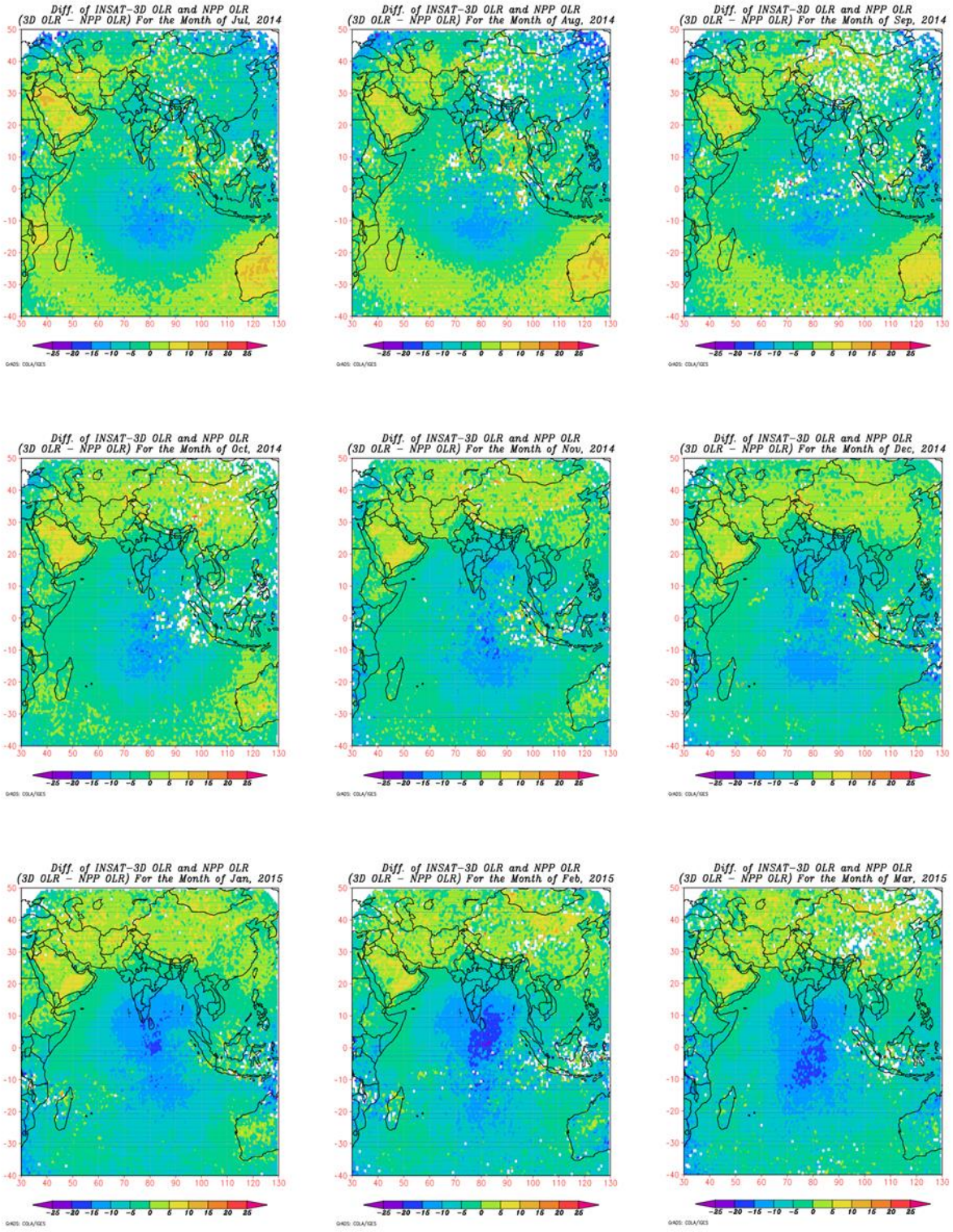

Fig. 6. Monthly Bias Plots between INSAT-3D, OLR and Suomi-NPP, CERES OLR (June 2014 to March 2015)

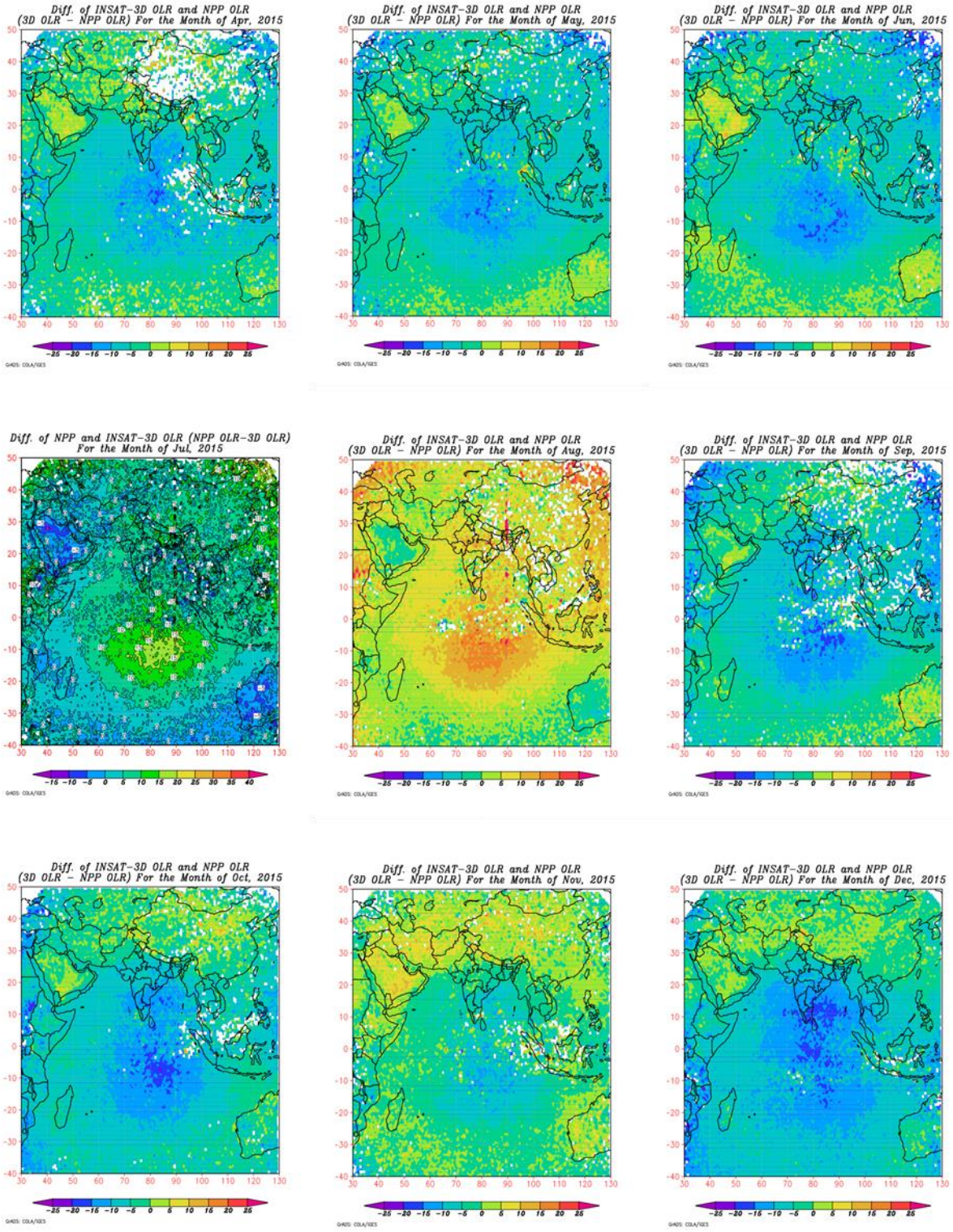

Fig. 6. Monthly Bias Plots between INSAT-3D, OLR and Suomi-NPP, CERES OLR (April 2015 to December 2015)

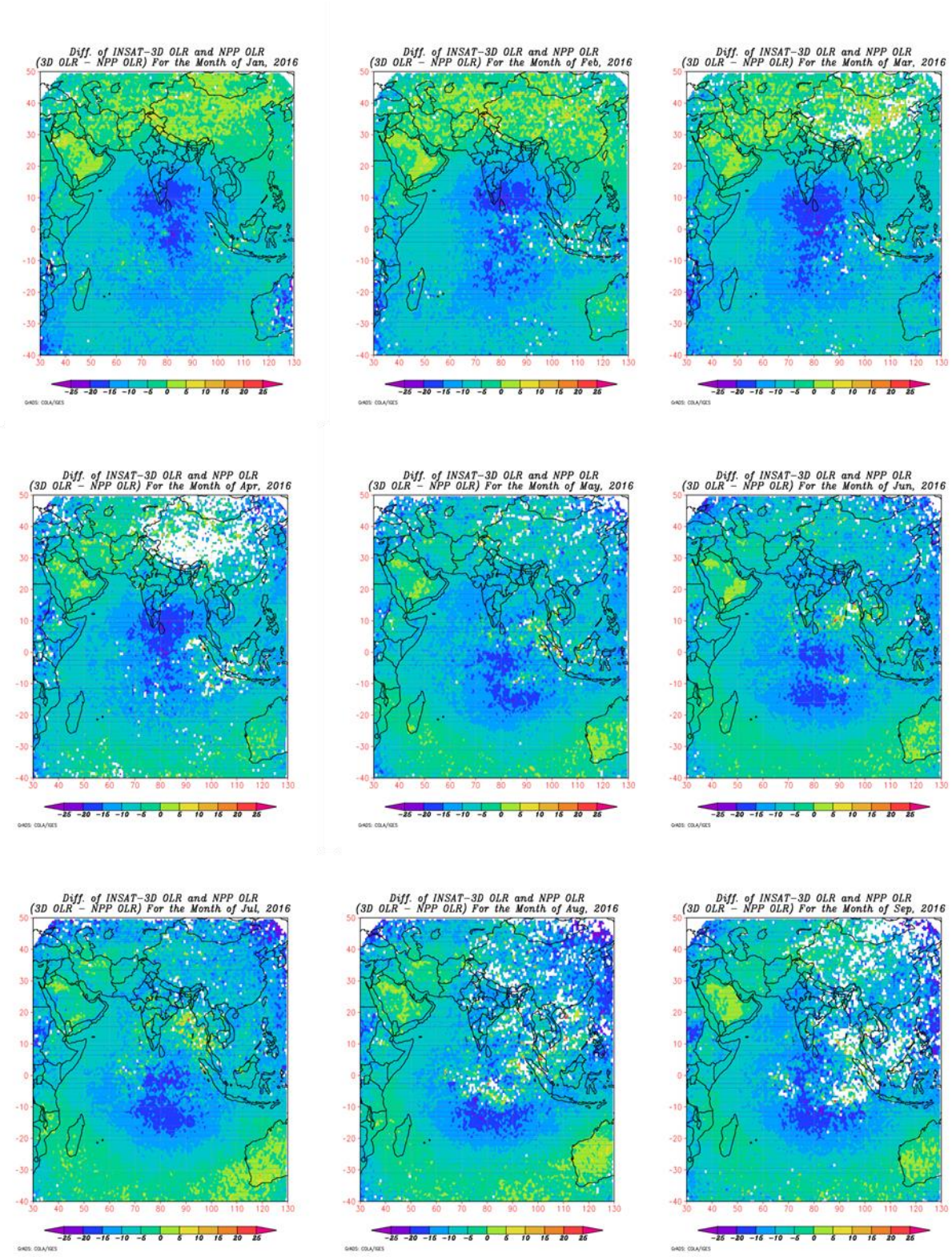

Fig. 6. Monthly Bias Plots between INSAT-3D, OLR & Suomi-NPP, CERES OLR (January 2016 to September 2016)

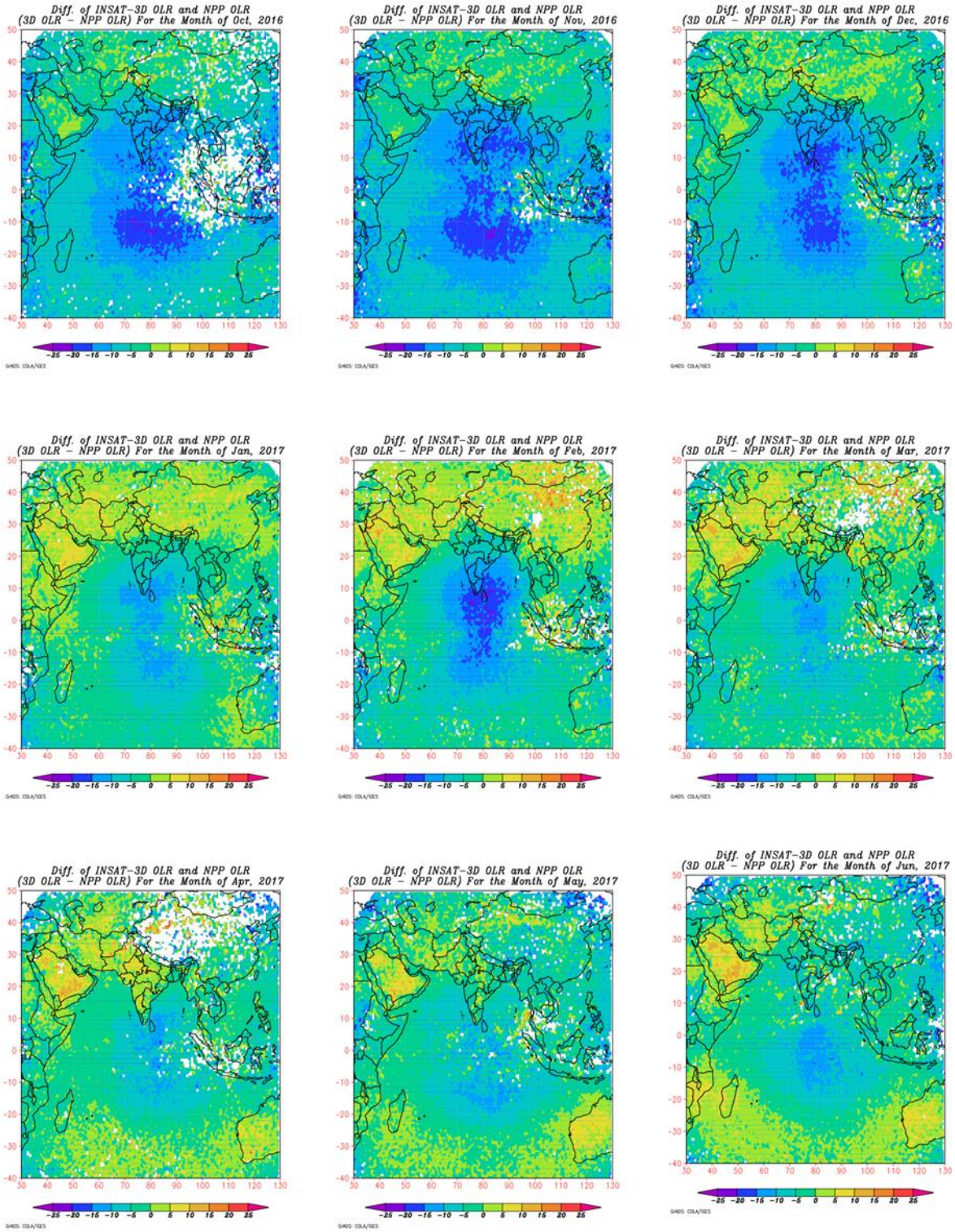

Fig. 6. Monthly Bias Plots between INSAT-3D, OLR & Suomi-NPP, CERES OLR (October 2016 to June 2017)

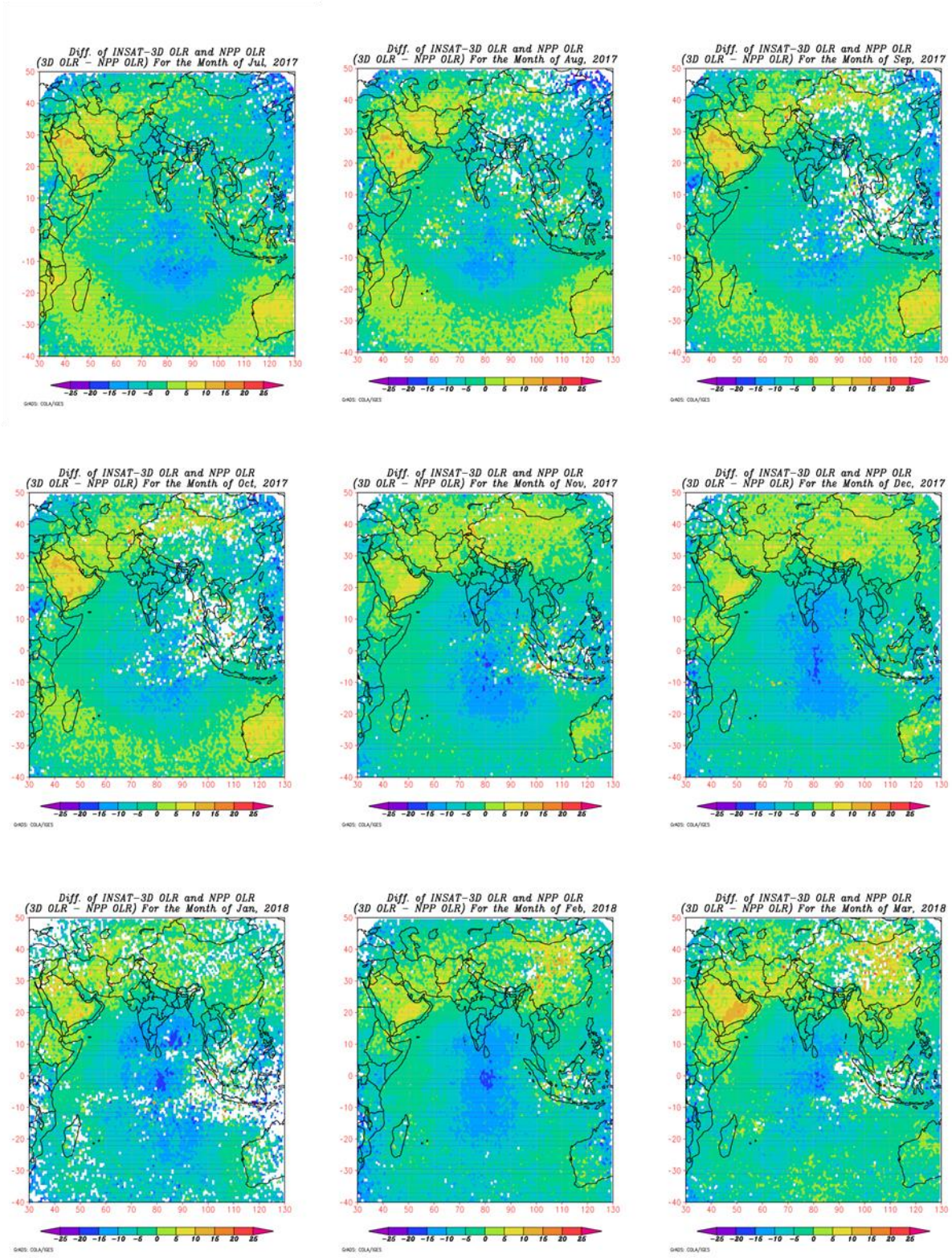

Fig. 6. Monthly Bias Plots between INSAT-3D, OLR & Suomi-NPP, CERES OLR (July 2017 to March 2018)

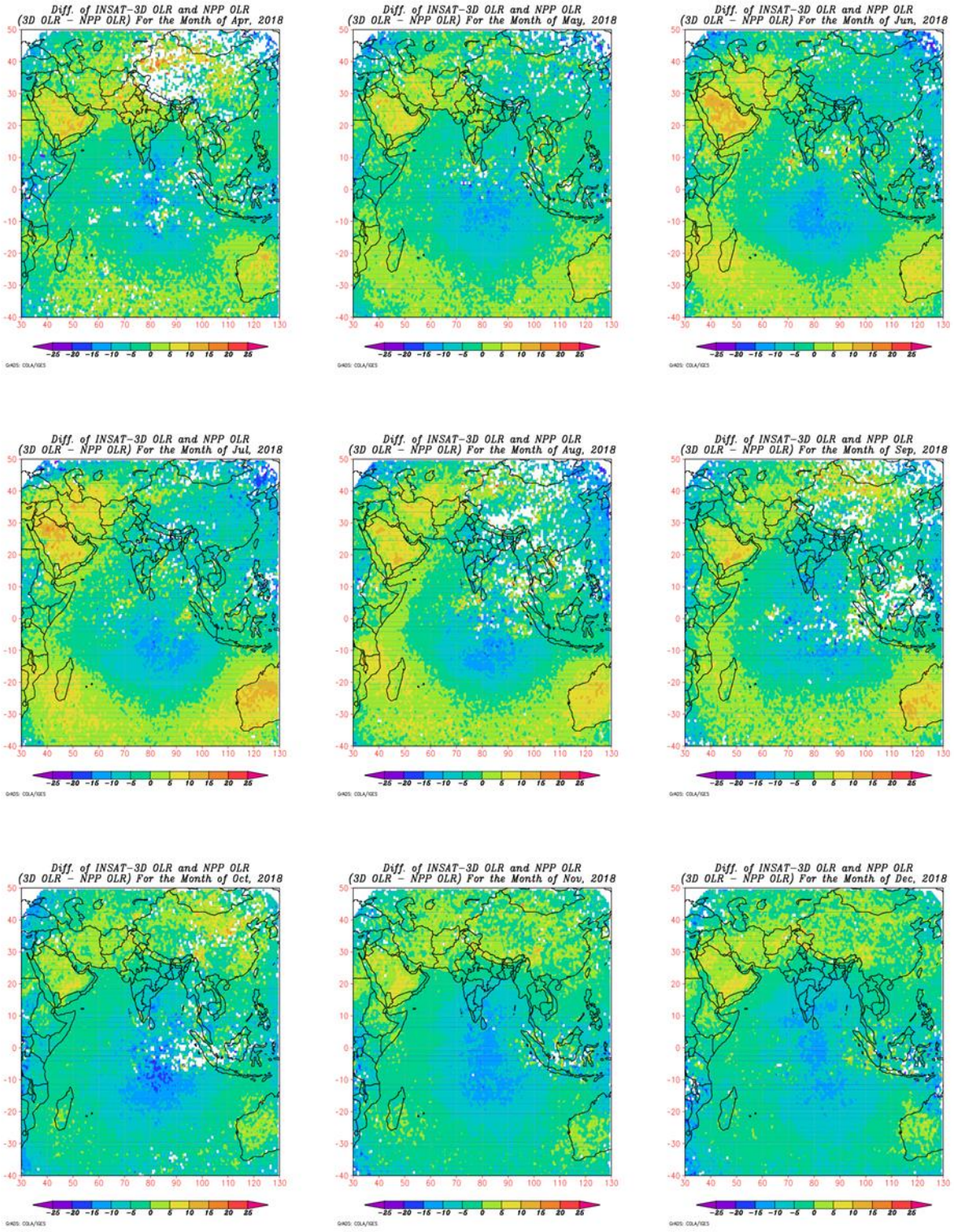

Fig. 6. Monthly Bias Plots between INSAT-3D, OLR & Suomi-NPP, CERES OLR (April 2018 to December 2018)

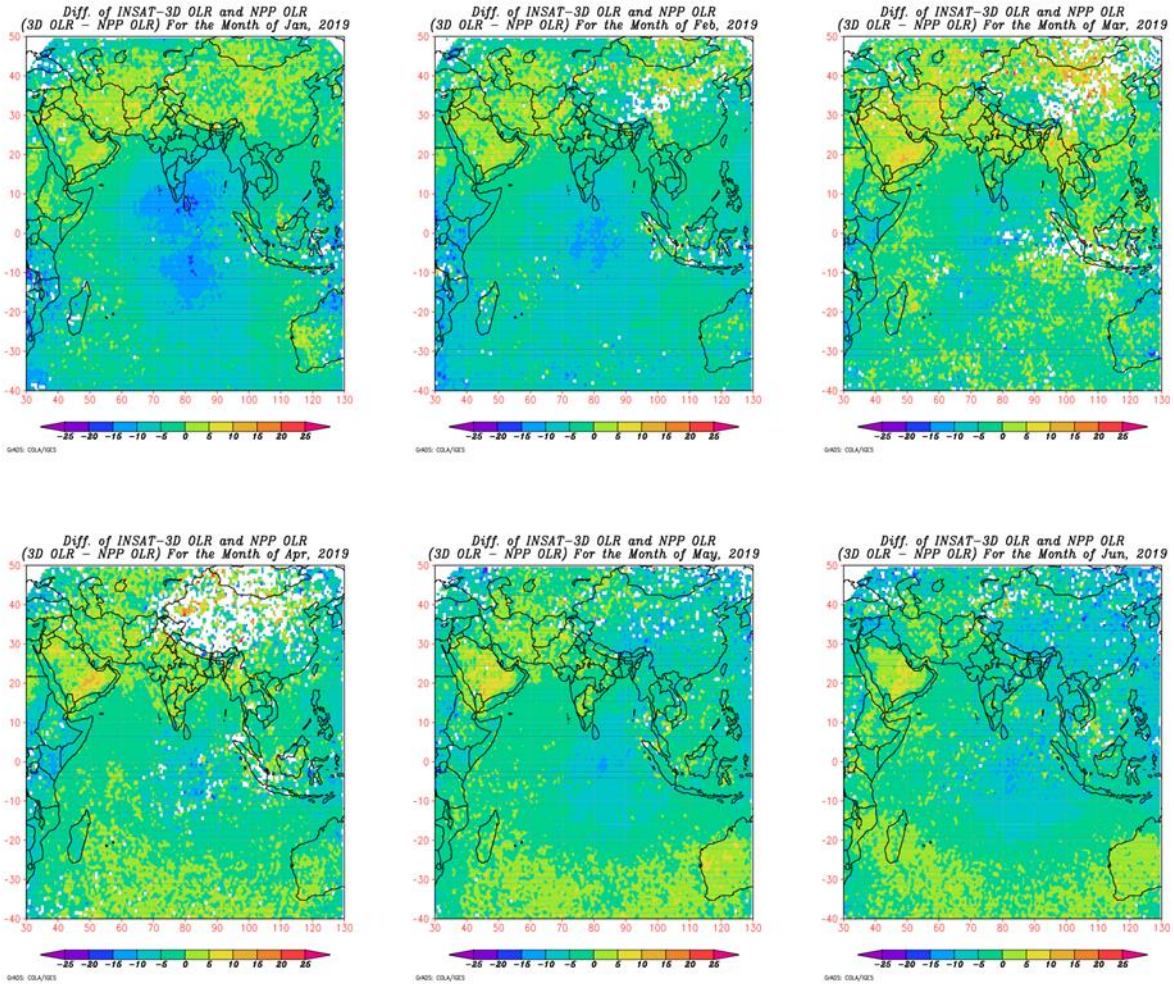

Fig. 6. Monthly Bias Plots between INSAT-3D, OLR & Suomi-NPP, CERES OLR (January 2019 to June 2019)